



# Dietary genistein increases microbiota-derived short chain fatty acid levels, modulates homeostasis of the aging gut, and extends healthspan and lifespan

Qihang Hou<sup>1</sup>, Jingxi Huang<sup>1</sup>, Lihua Zhao, Xianjie Pan, Chaoyong Liao, Qiuyu Jiang, Jiaqi Lei, Fangshen Guo, Jian Cui, Yuming Guo, Bingkun Zhang<sup>\*</sup>

State Key Laboratory of Animal Nutrition, College of Animal Science & Technology, China Agricultural University, Haidian District, Beijing 100193, China

## ARTICLE INFO

### Keywords:

Aging gut  
Genistein  
Healthspan  
*Lachnospira*  
Short-chain fatty acid  
Progeroid mice

## ABSTRACT

Age-related gastrointestinal decline contributes to whole-organism frailty and mortality. Genistein is known to have beneficial effects on age-related diseases, but its precise role in homeostasis of the aging gut remains to be elucidated. Here, wild-type aging mice and *Zmpste24*<sup>-/-</sup> progeroid mice were used to investigate the role of genistein in lifespan and homeostasis of the aging gut in mammals. A series of longitudinal, clinically relevant measurements were performed to evaluate the effect of genistein on healthspan. It was found that dietary genistein promoted a healthier and longer life and was associated with a decrease in the levels of systemic inflammatory cytokines in aging mice. Furthermore, dietary genistein ameliorated gut dysfunctions, such as intestinal inflammation, leaky gut, and impaired epithelial regeneration. A distinct genistein-mediated alteration in gut microbiota was observed by increasing *Lachnospira* abundance and short-chain fatty acid (SCFA) production. Further fecal microbiota transplantation and dirty cage sharing experiments indicated that the gut microbiota from genistein-fed mice rejuvenated the aging gut and extended the lifespan of progeroid mice. It was demonstrated that genistein-associated SCFAs alleviated tumor necrosis factor alpha-induced intestinal organoid damage. Moreover, genistein-associated propionate promoted regulatory T cell-derived interleukin 10 production, which alleviated macrophage-derived inflammation. This study provided the first data, to the authors' knowledge, indicating that dietary genistein modulates homeostasis in the aging gut and extends the healthspan and lifespan of aging mammals. Moreover, the existence of a link between genistein and the gut microbiota provides a rationale for dietary interventions against age-associated frailty.

## 1. Introduction

Early life mortality has been decreasing worldwide since the 1950 s, resulting in a dramatic increase in the aging population. It is predicted that the number of elderly people aged > 65 years will more than double and reach 1.5 billion in the next 30 years, which will lead to a sharp rise in the costs of healthcare worldwide [1]. Therefore, there is an urgent need to address the determinants of delayed age-related decline or healthspan in the elderly. Aging is inevitable, leading to an increased vulnerability to chronic diseases, multiple organ dysfunction, and pharmacological interventions [2]. Longevity can be promoted by virus factors, such as exercise, caloric restriction, and medication [3], but the relationship to healthspan, the disease-free and functional period

of life, is unclear [4]. The Frailty Index (FI) was developed to measure the healthspan in aging studies, which is critical for evaluating the aging state of mammals rather than just focusing on lifespan [5–7]. Using the FI, here, a series of longitudinal, clinically relevant healthspan measurements were undertaken to precisely evaluate health during an aging intervention. Although age-related characteristics are quite diverse, many studies have indicated that chronic low-grade inflammation is one of the most consistent biological features of aging [8–10]. Even in the absence of illness, elevated levels of inflammatory markers, such as interleukin-6 (IL-6) and tumor necrosis factor alpha (TNF- $\alpha$ ), have been consistently reported in aging population studies [11].

The mammalian gut is the core organ involved in nutrient digestion and absorption in the body. Intestinal health is closely related to the

<sup>\*</sup> Correspondence to: China Agricultural University, China.

E-mail address: [bingkunzhang@126.com](mailto:bingkunzhang@126.com) (B. Zhang).

<sup>1</sup> These authors contributed equally.

host's health status, defense system, and nutrition during the aging process [12]. A large amount of evidence has shown that gut aging is associated with a decline in gut function at both the organ and cellular levels, including impaired intestinal epithelial barrier function, immune function disorders, and gut dysbiosis [13,14]. Integrity of the intestinal epithelial barrier is crucial for health and to prevent disease. However, intestinal epithelial barrier functions decline in the elderly, leading to various issues, such as intestinal inflammation, leaky gut, intestinal stem cell (ISC) exhaustion, and impaired epithelial regeneration [12,14]. Moreover, an increased inflammatory state is a hallmark of gut aging [15]. Aging induces an imbalance between inflammatory and anti-inflammatory cytokines, favoring the excessive production of macrophage-derived IL-6 and TNF- $\alpha$  and directly affecting intestinal homeostasis [15,16].

Over the last few decades, emerging evidence has shown that the gut microbiota plays a critical role in the developmental programming of human health and disease. Age-related changes in gut microbiota composition include a decline in microbiota diversity, decreased abundance of beneficial microorganisms, increased abundance of potential pathogenic bacteria, and an increase in the ratio of Bacteroides to Firmicutes [12,17]. Moreover, the aging gut microbiota shows a loss of genes involved in the production of short-chain fatty acids (SCFAs) and secondary bile acids; a reduced representation of starch, sucrose, galactose, glycolysis, and gluconeogenesis metabolism pathways; and a concomitant loss of cellulolytic microorganisms [12,18].

Nearly a century of research has shown that nutritional intervention can delay aging and age-related diseases. Widely studied interventions include caloric restriction, protein restriction, and phytochemical supplements [3,19]. Natural polyphenols, which are found in commonly consumed food plants such as tea, cocoa, fruits and beans, exert many health benefits on aging [20]. For example, quercetin, resveratrol, and anthocyanin play important roles in the treatment of aging-related diseases [21–23]. Genistein, a polyphenol compound, belongs to the category of isoflavones, and has been found almost all leguminous plants including soybeans and coffee beans [24]. Many studies have indicated that genistein can alleviate inflammation, modify the gut microbiota, and improve epithelial barrier function in several animal models of intestinal diseases [25–28]. Moreover, genistein is known to have beneficial effects on age-related diseases, such as neurodegenerative and cardiovascular diseases, bone loss, and skin aging, but its precise role in homeostasis of the aging gut remains to be elucidated [29]. Laboratory mice, *Drosophila*, and *Caenorhabditis elegans* are common models for the study of aging and age-related diseases [30]. Previous studies have demonstrated that genistein prolongs the lifespan of *Drosophila* and *C. elegans* [31,32]. However, no systematic study concerning the lifespan- and healthspan-extending activity of genistein in mammals has been published, to the authors' knowledge.

The use of humans in aging research is complicated by many factors, including ethical issues, environmental and social factors, and perhaps most importantly, their long natural lifespan. Although cellular models of human diseases provide valuable mechanistic information, they are limited in that they may not replicate in vivo biology. Almost all organisms age; thus, animal models can be useful for studying aging [33]. In this study, wild-type (WT) aging mice and *Zmpste24*<sup>-/-</sup> progeroid mice were used to investigate the role of genistein in homeostasis of the aging gut. *Zmpste24*<sup>-/-</sup> progeria mice, which are characterized by gut dysbiosis and accelerated aging, are ideal models for studying the relationship between healthspan and gut microbiota [18]. Based on these animal models, the results of this study provided further evidence on age-associated frailty and mortality, gut dysbiosis, and intestinal physiology, providing valuable insights into how dietary genistein affects healthspan and lifespan, gut microbiota composition and functionality, intestinal epithelial barrier function, and biomarkers of inflammation in aging and progeria mammals. More importantly, considering the abundance of genistein in the human diet, the findings of this study point to a potential dietary intervention that improves the quality of life

in the elderly population. However, clinical longevity trials are required to establish the safety and efficacy of genistein in humans.

## 2. Materials and methods

### 2.1. Animals

Male C57BL/6 J (WT and specific pathogen-free [SPF]) mice were purchased from Vital River Laboratories (Vital River Laboratory Animal Technology Co. Ltd, Beijing, China) at 4 weeks of age. Progeroid *Zmpste24*<sup>+/-</sup> mice (SPF, C57BL/6 background) were purchased from the Shanghai Model Organisms Center, Inc. *Zmpste24*<sup>-/-</sup> mice were generated by crossing *Zmpste24*<sup>+/-</sup> mice. All mice were housed on a 12 h light / dark cycle and maintained at 20–22 °C with free access to food and water. All mice were maintained on a regular mouse diet (SPF, Beijing Keao Xieli Feed Co. Ltd) and sterile water. Genistein (absin) was homogeneously mixed during the manufacture of the regular mouse diet prior to irradiation and pelleting (400 mg genistein per 1 kg regular mouse diet). Genistein-treated animals were subjected to lifelong genistein supplementation in a regular mouse diet (400 mg/kg), while the control group was maintained on a regular mouse diet. C57BL/6 mice were fed regular chow and switched to a diet containing genistein at 18 months of age. The mice were housed in groups of four-to-five per cage. The mice were inspected daily, and treated for non-life-threatening conditions, as directed by veterinary staff. Health screening was performed four times per year at 3-month intervals. Diagnostics consisted of serological screening and fecal and fur analyses for internal and external parasites. Mice were maintained in accordance with the Guide for the Care and Use of Laboratory Animals (Institute for Learning and Animal Research at China Agricultural University; SYXK-2015–0028). All procedures were approved by the Chinese Agricultural University Laboratory Animal Welfare and Animal Experimental Ethical Committee (AW82402202–1–1).

### 2.2. Survival and aging index (FI)

The end point of the lifespan study was natural death, and the age at which the mice died was recorded. The protocol for assessing the mouse aging index was largely based on that of previous studies [6,7]. These assessments indicated age-associated deterioration of health and included evaluation of the animals' musculoskeletal system, respiratory system, signs of discomfort, ocular and nasal systems, vestibulocochlear / auditory systems, digestive system, urogenital system, body weight, and body surface temperature. A value of 0 was assigned if no sign of frailty was observed and the animal was healthy for that phenotype. Moderate and severe phenotypes were scored as 0.5 and 1, respectively. A loss of temperature and weight was scored using the standard deviation. Briefly, the average and standard deviations (STDEV) were calculated sex-specifically using the baseline datasets (data collected before the start of the treatment for mice aged 18 months). A decrease in temperature or weight within one STDEV was scored as 0, a decrease larger than one STDEV but smaller than two STDEV was scored as 0.5, and any decrease of more than two STDEV was scored as 1. All measurements were completely blinded to subjective assessments. All mice (18 months old) were scored before grouping, and all 31 scores were applied to assign animals into different groups. A balanced partitioning of mice was performed; for any given mouse in any given group, there were similar mice in all other groups. This allowed any outcome of the study to be more related to experiments or treatments than to the inherent properties of a group. The mice were housed in groups of four-to-five per cage.

### 2.3. Histological analysis

The mice were euthanized with CO<sub>2</sub>, the intestinal tissues were removed immediately, and the length of the intestine was measured. The

proximal colonic tissues (2 cm) were fixed in 4% paraformaldehyde in phosphate-buffered saline (PBS) and stored in 50% ethanol. Fixed tissues were embedded in paraffin using standard procedures. The blocks were sectioned (5  $\mu$ m) and analyzed using a hematoxylin and eosin staining kit (Beijing Leagene Biotechnology Co., Ltd.). Histological scoring of the colon was performed under the following criteria, as described previously [34,35]. Cell infiltration: occasional inflammatory cells in the lamina propria (LP) = 0, increased infiltration in the LP predominantly at the base of crypts = 1, confluence of inflammatory infiltrate extending into the mucosa = 2, and transmural extension of infiltrate = 3; tissue damage: no mucosal damage = 0, partial (up to 50%) loss of crypts in large areas = 1, partial-to-total (50–100%) loss of crypts in large areas and epithelium intact = 2, and total loss of crypts in large areas and epithelium lost = 3. Histological scoring was performed in a blinded fashion.

#### 2.4. Intestinal permeability assay

The intestinal permeability assay was performed as described in the authors' previous study [36]. Briefly, mice were denied access to food but allowed water for 3 h prior to gavage with 0.2 mL saline containing 8 mg fluorescein isothiocyanate (FITC) and 70 kDa dextran (Sigma). The serum was harvested after 5 h and added to enzyme-linked immunosorbent assay (ELISA) plates (NEST Biotechnology). FITC fluorescence was measured at excitation wavelengths of 495 and 555 nm.

#### 2.5. DNA extraction and 16 S rRNA gene sequencing

Fecal DNA was extracted using a QIAamp DNA Stool Mini Kit (Qia-gen, Germany). The V3–V4 variable regions of intestinal bacterial 16 S DNA were amplified using universal primers of the forward 338 F (5'-ACTCCTACGGGAGGAGCAG-3') and reverse 806 R (5'-GGAC-TACHVGGGTWCTAAT-3'). Each sample was labeled with a unique barcode using a polymerase chain reaction (PCR). The PCR product was separated on a 2% agarose gel, and the relative concentration of the target band was measured. PCR products of equal quality from each sample according to their relative concentrations were pooled together to build a library. Sequencing was performed on an Illumina MiSeq platform (San Diego, CA, USA), according to the manufacturer's instructions, to generate paired-end reads of 250 bases.

#### 2.6. Microbiota data analysis

Raw paired-end reads were processed using the QIIME 2 platform (version 2020.2) [37]. Sequence quality controls were performed using DADA2: raw reads were filtered, trimmed, denoised, and dereplicated; forward and reverse sequences were merged; and chimeras were removed. Determinations of alpha and beta diversities were also conducted using QIIME 2. Alpha diversity and statistical data were calculated using the Shannon index. Beta diversity was measured using Bray–Curtis dissimilarity. Differentially abundant genera between groups were identified using linear discriminant analysis effect size (LEfSe) [38]. Predictions of the Kyoto Encyclopedia of Genes and Genomes (KEGG) metabolic pathways of the microbiota data were made using Tax4Fun [39]. Bar plots and correlations between differentially presented bacterial taxa and concentrations of cytokines or SCFAs were calculated using Spearman's correlation analysis.

#### 2.7. Fecal microbiota transplant

Fecal microbiota transplants (FMTs) were largely performed according to the methods of a previous study [18]. The effects of the FMTs were assessed using four different groups of progeroid mice: untransplanted *Zmpste24*<sup>-/-</sup> mice; *Zmpste24*<sup>-/-</sup> mice transplanted with empty buffer; *Zmpste24*<sup>-/-</sup> mice transplanted with fecal microbiota from aged control WT mice; and *Zmpste24*<sup>-/-</sup> mice transplanted with fecal

microbiota from genistein-fed WT mice. Eight-week-old *Zmpste24*<sup>-/-</sup> mice were used as recipients. Before transplantation, *Zmpste24*<sup>-/-</sup> mice were administered 100  $\mu$ L of an antibiotic cocktail (1 g l<sup>-1</sup> neomycin, 1 g l<sup>-1</sup> vancomycin, 2 g l<sup>-1</sup> ampicillin, and 2 g l<sup>-1</sup> metronidazole) by oral gavage for five consecutive days. Subsequently, mice were administered 100  $\mu$ L of the microbiota suspension twice a week for 1 month. After this 1-month period, the mice received the microbiota suspension once a week until natural death or euthanasia. For the microbiota suspension preparation, fresh feces pellets (30–60 mg of feces per mice) were collected from control or genistein-fed aging mice from every cage in the euthanasia group (n = 8, Fig. 1A) and resuspended with a homogenizer in reduced PBS with 0.5 g l<sup>-1</sup> cysteine and 0.2 g l<sup>-1</sup> Na<sub>2</sub>S (200 mg of feces per 1 mL of PBS) to avoid cage effects. The fecal homogenate was then filtered through a 40  $\mu$ m cell strainer (Jet Biofil). The filtrate was centrifuged at 500  $\times$  g for 1 min to remove insoluble material, and 100  $\mu$ L of the supernatant was administered to the mice by oral gavage. The mice in the empty transplant group received the same antibiotic treatment and were transplanted with reduced PBS only.

#### 2.8. Dirty cage-sharing experiment

Dirty cage-sharing experiments were performed according to the methods of a previous study [40]. Dirty cages containing feces and bedding from age-matched controls or genistein-fed aged mice in the euthanasia group (Fig. 1A) were collected every week. Eight-week-old SPF *Zmpste24*<sup>-/-</sup> mice (recipients) were kept in dirty cages and transferred to new dirty cages weekly over a span of 8 weeks.

#### 2.9. Quantification of SCFA profiles

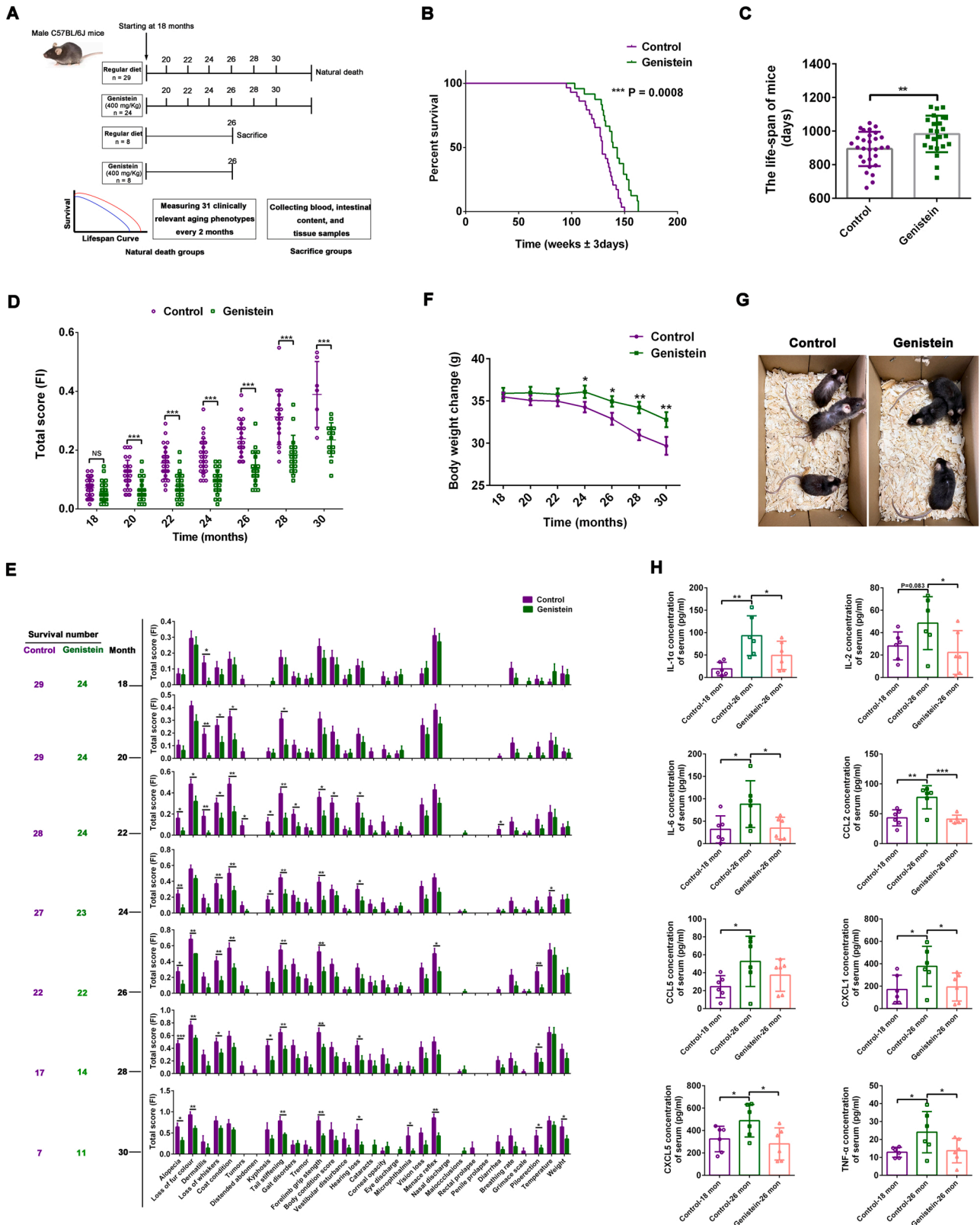
SCFAs, including acetate, propionate, butyrate, valerate, isobutyrate, and isovalerate, in fecal samples or culture medium of *Lachnospiraceae* (purchased from BeNa Culture Collection) were quantified using gas chromatography (GC2010pro, Shimadzu, Japan). Briefly, 100 mg of fecal samples was weighed, homogenized in sterile PBS (1:5), and then centrifuged at 3000  $\times$  g for 10 min. The supernatant was filtered through a 0.22  $\mu$ m sterile membrane, kept in a 2 mL screw-cap vial, and then subjected to SCFA analysis with an Ion Chromatography System.

#### 2.10. ELISA

A portion of frozen colonic tissues (1 cm) was harvested and homogenized in 0.5 mL of radioimmunoprecipitation assay lysis buffer (Shanghai WellBio technology Co., Ltd, WB0101) with 1 mM phenylmethylsulfonyl fluoride (Life-iLab, China). Samples were then centrifuged for 15 min at 12,000  $\times$  g. Total protein was extracted using the InniExt™ Mammalian Total Protein Extraction Kit (InniBio.GuangZhou). The protein concentration was quantified using a PikoOrange Protein Quantitation Kit (Life-iLab, China). The supernatant (0.5 mg protein in 0.1 mL) was assayed for cytokines. Cytokines in the supernatant and serum were detected using mouse IL-1 $\alpha$  (BlueGene), IL-2 (Boster), IL-1 $\beta$  (Jiangsu Meimian industrial Co., Ltd), IL-6 (Shanghai Zcibio Technology Co. Ltd.), IL-4 (NeoBioscience), IL-10 (FineTest), IL-13 (ShenZhen ZiKer Biological Technology Co. Ltd), IL-15 / IL-15 $\alpha$  (Invitrogen™), IL-17 (Invitrogen™), IL-22 (Jianglaibio), TNF- $\alpha$  (Xinyu Biology), C-C motif chemokine ligand 2 (CCL2) (RD systems), CCL5 (RD systems), C-X-C motif chemokine ligand 1 (CXCL1) (RD systems), and CXCL5 (RD systems) ELISA kits, according to the manufacturer's instructions.

#### 2.11. Immunofluorescence assay

Sections of the colon (2 cm each) were collected from mice in different groups, fixed overnight in 4% paraformaldehyde, embedded in optimal cutting temperature compound, cut into 8  $\mu$ m-thick slices, and rinsed in Hanks' balanced salt solution (HBSS). Tissue sections were



(caption on next page)

**Fig. 1.** Dietary genistein extends the lifespan and alleviates age-associated frailty in aging mice. (A) Experimental design, related to Figs. 1–3. The male C57BL/6 J mice were fed genistein (400 mg/kg) or a standard diet at 18 months of age. The study consisted of two natural death groups (Control [n = 29] and Genistein [n = 24]) and two sacrifice groups (Control [n = 8] and Genistein [n = 8]). Mice in the natural death groups were used for measuring 31 clinically relevant aging phenotypes and the lifespan, and were also used for collecting blood, intestinal content, and tissue samples. (B) Survival proportions of the Control (n = 29) and Genistein (n = 24) mice. Survival curve comparisons were performed using the Log-rank test; \* \*\*p < 0.001. (C) The lifespan of the Control (n = 29) and Genistein (n = 24) mice. Data are the mean  $\pm$  standard deviation (SD) of the group, \* \*\*p < 0.01 (two-tailed t test). (D) Total frailty index scores during the lifespan, comparing control mice to those fed genistein from 18 months of age. Each dot indicates the total score of one animal at a specific age as indicated; n = all live animals in the study at each time point. Data are the mean  $\pm$  SD, \* \*\*p < 0.001 (two-tailed t-test). (E) All individual frailty phenotypes (total of 31 phenotypes), n = all animals alive at each measurement time. Data are the mean  $\pm$  SD, \* p < 0.05, \* \*p < 0.01, \* \*\*p < 0.001 (two-tailed t-test). (F) Body weight trajectories of Control and Genistein mice; n = all live animals in the study at each time point. Data are the mean  $\pm$  SD, \* p < 0.05, \* \*p < 0.01 (two-tailed t-test). (G) Age-matched control (left) and genistein-fed (right) mice. Animals were 26 months old in the image. (H) The expression of eight cytokines from the serum of the middle-aged control (18 months old), aged control (26 months old), and genistein-fed (26 months old) mice (n = 6). Data are the mean  $\pm$  SD, \* p < 0.05, \* \*p < 0.01, \* \*\*p < 0.001 (one-way analysis of variance).

permeabilized with 0.5% Triton X-100 for 20 min, washed three times with HBSS, and incubated for 1 h in 5% bovine serum albumin in HBSS to reduce nonspecific background signals. For immunofluorescence staining, tissue sections were incubated overnight with primary antibodies (anti-Ki-67, 1:50; ZENBIO, 261202). The samples were then incubated with DyLight 594 (1:200, Abcam, ab150080)-conjugated secondary antibodies for 1 h, followed by incubation with 4',6-diamidino-2-phenylindole (1:5000, Invitrogen™, D1306) for 5 min at 25 °C. The mean fluorescence intensity (MFI) of Ki-67 or Muc2 was analyzed using ImageJ software.

## 2.12. Mouse intestinal organoid culture

Colonic organoid culture was performed according to the methods of the authors' previous studies [35,41]. Briefly, colon tissues were removed immediately after euthanizing mice with CO<sub>2</sub>. Organs were opened longitudinally in a 100 mm cell culture dish (CellVis), washed with sterile PBS, and cut into pieces. Colon pieces were incubated in colonic crypt isolation buffer (5.6 mM Na<sub>2</sub>HPO<sub>4</sub>, 8 mM KH<sub>2</sub>PO<sub>4</sub>, 9.8 mM NaCl, 1.6 mM KCl, 44 mM sucrose, 24.8 mM D-sorbitol, 5 mM ethylenediaminetetraacetic acid [EDTA], and 0.5 mM DL-dithiothreitol in distilled water) in 50 mL tubes (LABLEAD Inc.). The mixture was passed through a 70  $\mu$ m cell strainer, and the colonic crypt fractions were isolated and purified by centrifugation. Matrigel (VivaCell, VitroGel® ORGANOID, VHM04-K) was added to a pellet of crypt fractions, and 50  $\mu$ L drops of crypt-containing Matrigel were added to the wells of a 24-well plate. For colonic organoid culture, IntestiCult™ Organoid Growth Medium (STEMCELL) supplemented with epidermal growth factor (Novoprotein) was used. The culture medium was replaced every 3–4 days.

## 2.13. Regulatory T cell and macrophage isolation and culture

Colon tissues were collected from the mice, opened longitudinally, and washed with PBS. Epithelial cells were removed by incubating with Dulbecco's phosphate-buffered saline containing 5 mM EDTA, 0.154 mg/mL dithiothreitol, 5% fetal bovine serum (FBS) (Shanghai Lian Shuo Biotechnology Co., Ltd.), and 100 U/mL penicillin-0.1 mg/mL streptomycin for 30 min in a 37 °C shaker. For the isolation of LP lymphocytes (LPLs), the remaining intestinal tissues were washed twice in PBS, cut into 1 mm-long sections, and digested in a collagenase solution (Roswell Park Memorial Institute [RPMI] 1640 medium, 10 mM 4-[2-hydroxyethyl]-1-piperazineethanesulfonic acid, 100 U/mL penicillin-0.1 mg/mL streptomycin, 1% glutamine, 5% certified FBS [VivaCell, Shanghai], 0.5 mg/mL collagenase/dispase [Roche], 1 U/mL DNase 1 [Roche], and 0.5 mg/mL enterokinase [Hangzhou Putai Biotechnology Co., LTD]) for 30 min in a 37 °C shaker. The digested tissues were strained (40  $\mu$ m) and washed twice with PBS. The LPL fractions were purified using a 40% / 80% Percoll gradient (Solarbio). To sort regulatory T (T<sub>reg</sub>) cells and macrophages, colonic LPLs were obtained from six mice per sorting session. T<sub>reg</sub> cells (CD4<sup>+</sup>CD25<sup>+</sup>) were isolated from the LPL suspension using a CD4<sup>+</sup>CD25<sup>+</sup> T<sub>reg</sub> cell Isolation

Kit (Miltenyi, 130–092–984) according to the manufacturer's instructions. To activate and maintain T<sub>reg</sub> cells in culture, anti-CD3 (1 g/mL; Bioss), anti-CD28 (1 g/mL; Sangon biotech), and mIL-2 (1000 U/mL; CUSABIO, <https://www.cusabio.com/>) were added to the complete RPMI 1640 medium (BioChannel Biological Technology Co., Ltd.). In some experiments, T<sub>reg</sub> cells were stimulated with genistein (0.1 mM), acetate (1 mM), propionate (1 mM), butyrate (1 mM), or anti-IL-10 antibody (1  $\mu$ g/mL; BOSTER) for 24 h. Macrophages (F4 / 80<sup>+</sup> cells) were isolated from the LPL suspension using the Macrophage Isolation Kit (Miltenyi, 130–110–434) according to the manufacturer's instructions. To stimulate macrophages, cells were incubated with 100 ng/mL lipopolysaccharide. The cell samples and their culture supernatants were harvested for flow cytometry and ELISA.

## 2.14. Flow cytometry

To assess the frequency of apoptosis (Annexin V / propidium iodide) and proliferating (5-ethynyl-2'-deoxyuridine [EdU]) cells in colonic organoids, single cells were isolated from organoids incubated in 1  $\times$  TrypLE express (Beijing T&L Biological Technology Co., Ltd.) supplemented with 0.8 kU mL<sup>-1</sup> DNase1 (Roche). Single cells were stained using an Annexin V-FITC Apoptosis Detection Kit (Beyotime). Single cells were fixed with 4% paraformaldehyde. After obtaining a single-cell suspension of stimulated and fixed cells, the samples were filtered (40  $\mu$ m) and permeabilized with ice-cold (–20 °C) methanol. The fixed and permeabilized cells were rehydrated with PBS, thoroughly washed with PBS before staining, and stained using a Cell-Light EdU DNA Cell Proliferation Kit (Shanghai Zcibio Technology Co. Ltd.).

For surface marker staining, cells were stained with anti-mouse CD3 APC (17A2, BD Pharmingen™, 565643), anti-mouse CD4 Pacific Blue (RM4–5, BD Pharmingen™, 558107), anti-mouse CD25 APC (3C7, BD Pharmingen™, 558643), anti-mouse CD11b PE-Cy7 (M1/70, BioLegend, 101216), anti-mouse CD11b Pacific Blue (M1/70, BioLegend, 101224), and anti-mouse CD11c FITC (N418, BioLegend, 117305) antibodies. For intracellular cytokine staining, T<sub>reg</sub> cells or macrophages were stimulated with PMA (50 ng/mL) and ionomycin (1000 ng/mL) in the presence of Brefeldin A (5  $\mu$ g/mL; Molnova Chemicals [Shanghai, China]) for 6 h. The cells were fixed, permeabilized, and stained with anti-mouse IL-6 PE (MP5–20F3, BioLegend, 504503), anti-mouse IL-10 PE (JES5–16E3, BioLegend, 505007), anti-mouse IL-10 PE-Cy7 (JES5–16E3, BioLegend, 505025), and anti-mouse TNF- $\alpha$  PE (MP6–XT22, BioLegend, 506305) antibodies. To analyze intracellular signaling in T<sub>reg</sub> cells, sorted colonic T<sub>reg</sub> cells were fixed with a Fixation/Permeabilization Solution Kit (BD) and stained with anti-mouse ROR $\gamma$ t FITC (Q21–559, BD Pharmingen™, 563621) and anti-mouse GATA-3 PE (L50–823, BD Pharmingen™, 560074) antibodies. Samples were detected with a BD FACSCanto™ II (BD) and analyzed with FlowJo software, with isotype or unstained controls to determine the gating.

## 2.15. Quantitative reverse transcription PCR

Total RNA from the intestinal tissues, contents, and organoids was

extracted using an automated nucleic acid extractor (Scientz-NP-2032). Reverse transcription of RNA was performed using an *Evo M-MLV RT Kit* (Accurate Biotechnology [Hunan] Co. Ltd.). Then, 2  $\mu$ L of template RNA was reacted with SYBR PCR Master Mix (Genstar) for a final volume of 20  $\mu$ L. Reagents were added to 96-well PCR plates (NEST Biotechnology). The thermal cycling conditions were as follows: 5 min at 95 °C, followed by 40 cycles of 15 s at 95 °C and 34 s at 60 °C using an Applied Biosystems 7500 real-time PCR system. The primers used are listed in Table 1.

### 2.16. Statistical analysis

The results are expressed as mean  $\pm$  SD from two or three independent experiments, unless otherwise stated. One-way analysis of variance was used to identify significant differences among multiple groups, and the *t*-test was used to identify significant differences between the two groups. For nonparametric distributions, Wilcoxon rank-sum and Kruskal–Wallis tests were performed for comparisons between two groups or three or more groups, respectively. Survival analysis was performed using the Kaplan–Meier method, and statistical differences were analyzed using the Log-rank (Mantel–Cox) test (GraphPad Prism 6.0 and survival R package).

### 2.17. Availability of data and materials

Data supporting the findings of this study are available from the corresponding author upon reasonable request. The datasets supporting the conclusions of this article are available from the NCBI Sequence Read Archive repository under accession numbers PRJNA872038 and PRJNA872108.

## 3. Results

### 3.1. Dietary genistein extends the lifespan and alleviates age-associated frailty in aging mice

To assess the efficacy of genistein on longevity, male C57BL/6 J mice were subjected to lifelong genistein supplementation (400 mg/kg normal chow diet) at 18 months of age (Fig. 1A). Interestingly, genistein-fed mice showed improved survival compared to control mice, with a 9.3% increase in median lifespan (987 vs. 903 days, respectively) and a 9.2% increase in maximum lifespan (1144 vs. 1048 days, respectively) (Fig. 1B and Table 2). Genistein-fed mice also exhibited a 10.0% increase in mean lifespan (983 versus 894 days, respectively) (Fig. 1C and Table 2). A clinically relevant FI consisting of 31 phenotypes has been widely used to assess healthspan in the field of aging research [6,7,42]. The total frailty score, which is the average of 31 frailty phenotypes, was calculated for each animal at every time point (Fig. 1D) and indicated a state of increased vulnerability to adverse health outcomes comparable to morbidity. It was demonstrated that genistein decreased the incidence and severity of the aging phenotypes and delayed morbidity (Fig. 1D). Moreover, genistein treatment decreased the severity of multiple age-dependent phenotypes, including poor coat condition, fur color loss, and tail stiffening (Fig. 1E). Genistein treatment did not improve these phenotypes. However, no significant adverse effects were detected following genistein treatment (Fig. 1E).

**Table 1**

Primer sequences used for qRT-PCR.

Target genes	Primer sense (5'–3')	Primer antisense (5'–3')	Product size (bp)
mLgr5	CCTACTCGAAGACTTACCCAGT	TGCATTGGGGTGAATGATAGCA	165
mAscl2	CGCTCTCTGCCTCCTACCT	GTCCGAGAGAGGGTCCGAAT	164
mp16	TGGTCACTGTGAGGATTCAGC	GTTGCCATCATCATCACCTGG	192
mp21	TATCCAGACATTACAGAGCCACA	CACGGGACCGAAGAGACAAC	100
mGAPDH	GGCTGTATTCCCCTCCATCG	CCAGTTGGTAACAATGCCATGT	154

**Table 2**

The effect of genistein treatment on lifespan.

		Median lifespan	Mean lifespan	Maximum lifespan
Wild-type aging mice	Control (days)	903	894	1048
	Genistein (days)	987	983	1144
	Percentage extension (%), Genistein vs. Control)	9.3%	10.0%	9.2%
<i>Zmpste24</i> <sup>-/-</sup> progeroid mice	Control (days)	182	172	220
	ET (days)	182	179	223
	A-FMT (days)	144	133	194
	GA-FMT (days)	217	211	293
	Percentage extension (%), A-FMT vs. Control)	-20.9%	-29.3%	-11.8%
	Percentage extension (%), GA-FMT vs. Control)	19.2%	22.7%	33.2%
	Percentage extension (%), GA-FMT vs. A-FMT)	50.7%	58.6%	51.0%

Moreover, genistein-fed mice manifested delayed loss of body weight (Fig. 1F) and visible signs of aging (Fig. 1G). Age-associated diseases are accompanied by chronic low-grade inflammation, which is defined as ‘inflammaging’ [43]. Inflammaging is characterized by increased levels of blood inflammatory markers that indicate high susceptibility to chronic frailty, morbidity, and premature death [11]. The levels of critical inflammation-related cytokines were measured in the sera of middle-aged control (18 months old), aged control (26 months old), and genistein-fed (26 months old) mice. In aged control mice, the levels of most pro-inflammatory cytokines (IL-1 $\alpha$ , IL-2, IL-6, TNF- $\alpha$ , CCL2, CCL5, CXCL1, and CXCL5) were higher than those in the middle-aged control mice (Fig. 2H). However, genistein treatment for 8 months reduced the levels of a large proportion of pro-inflammatory cytokines (IL-1 $\alpha$ , IL-2, IL-6, TNF- $\alpha$ , CCL2, CCL5, CXCL1, and CXCL5) in aged animals (Fig. 2H). Collectively, these findings demonstrated that dietary genistein extended the lifespan and alleviated age-associated frailty in aging mice.

### 3.2. Dietary genistein ameliorates gut dysfunction in aging mice

Aging is associated with alterations in gut functions, including intestinal inflammation, leaky gut, ISC exhaustion, and impaired epithelial regeneration [12,14]. Here, it was found that aging mice exhibited enhanced intestinal permeability (Fig. 2A) and increased histological scores of the colon (Fig. 2B) compared with middle-aged mice. Interestingly, genistein treatment decreased intestinal permeability (Fig. 2A) and reduced the histological scores of the colon (Fig. 2B) in aging mice compared with controls. Previous studies have shown the accumulation of senescent cells in different tissues of aging mice [44]. Cyclin-dependent kinase inhibitors p21 and p16 are markers of cellular senescence in various tissues [44]. Therefore, here, senescent markers in different tissues of mice were examined, and no significant changes in those of the heart, liver, lungs, or kidneys were detected (Fig. S1A–1D). Nevertheless, mRNA levels of *p16* and *p21* were downregulated in the colon of genistein-fed mice compared to those in the colon of the control

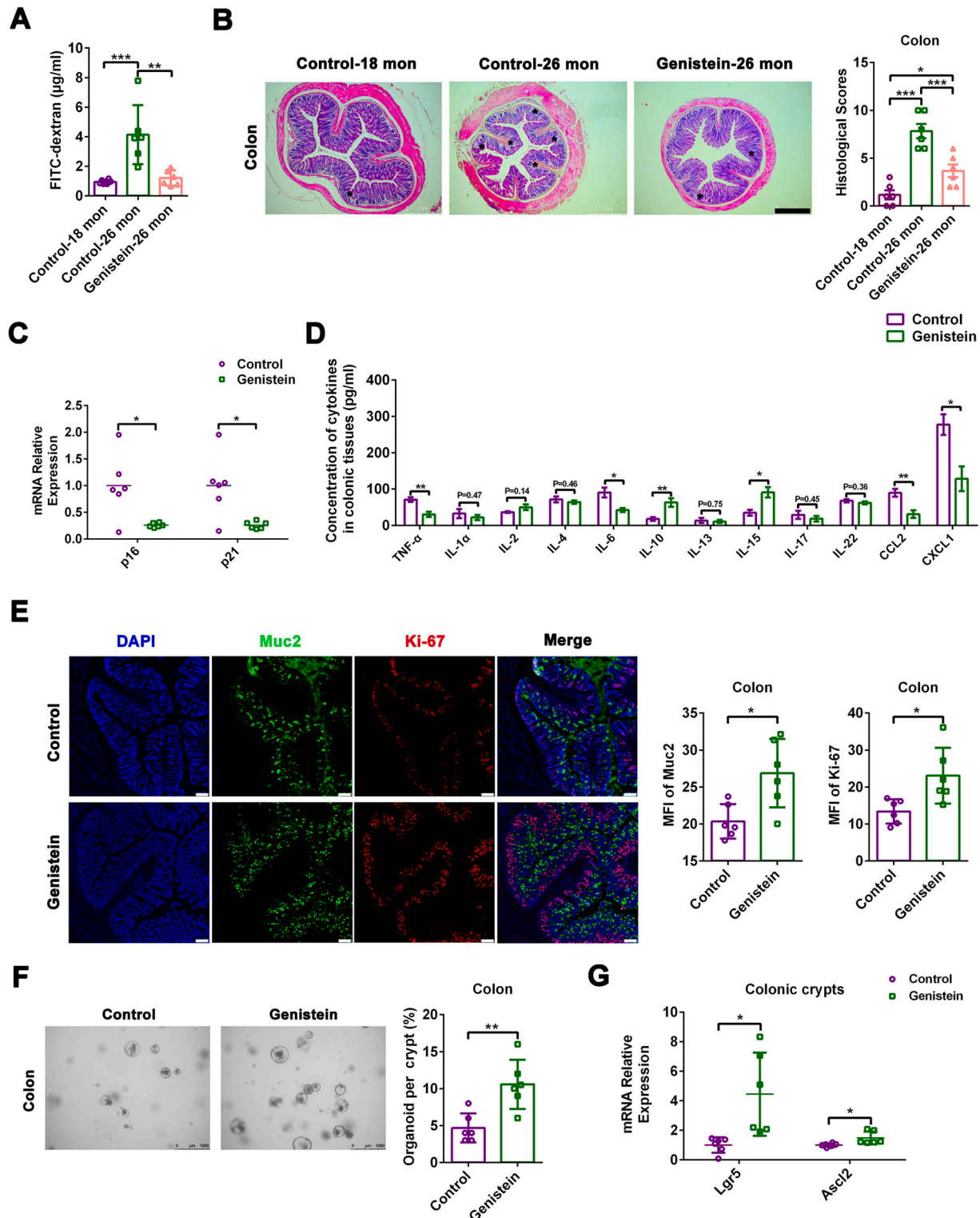


**Fig. 2.** Dietary genistein ameliorates gut dysfunction in aging mice. (A, B) Fluorescein isothiocyanate-dextran concentration from the serum (A) and representative histological images and scores of the colon (B) of middle-aged control (18 months old), aged control (26 months old), and genistein-fed (26 months old) mice (n = 6, asterisks mark inflammatory sites); scale bar, 1000 µm. Data are the mean ± standard deviation (SD), \*p < 0.05, \*\*p < 0.01, \*\*\*p < 0.001 (one-way analysis of variance). (C) Reverse transcription quantitative polymerase chain reaction (qRT-PCR) analysis of the markers of cellular senescence (*p16* and *p21*) of the colon from aged control (26 months old) and genistein-fed (26 months old) mice (n = 6). Data are the mean ± SD, \*p < 0.05 (two-tailed t-test). (D) The expression of 12 cytokines of the colon (n = 4). Data are the mean ± SD, \*p < 0.05, \*\*p < 0.01 (two-tailed t-test). (E) Immunostaining of Ki-67 (red), Muc2 (green), and 4',6-diamidino-2-phenylindole (blue) of the colon (n = 6); scale bar, 100 µm. Data are the mean ± SD, \*p < 0.05 (two-tailed t-test). (F) Organoid frequency of colonic crypts (n = 6); scale bar, 1000 µm. Data are the mean ± SD, \*\*p < 0.01 (two-tailed t test). (G) qRT-PCR analysis of the markers of ISCs (*Lgr5* and *Ascl2*) of colonic crypts (n = 6). Data are the mean ± SD, \*p < 0.05 (two-tailed t-test).

mice (Fig. 2C). Moreover, genistein treatment inhibited the expression of pro-inflammatory cytokines (TNF- $\alpha$ , IL-6, CCL1, and CXCL1), but enhanced the expression of the anti-inflammatory cytokine (IL-10) in the colonic tissues of aging mice (Fig. 2D). The mucus layer overlying the epithelium is secreted by goblet cells, which represent the first line of defense against physical and chemical injury [45]. Genistein treatment increased the expression of Muc2 in the colons of aging mice compared to in the colons of the control mice (Fig. 2E). The intestine is constantly challenged and requires a high renewal rate that relies on ISCs to replace damaged cells to maintain its barrier function [46]. Subsequently, whether genistein accelerates intestinal epithelial regeneration in aging mice was assessed. Interestingly, the number of Ki-67<sup>+</sup> proliferating cells increased in the colons of genistein-fed mice (Fig. 2E). Moreover, genistein treatment resulted in more crypt-formed organoids in aging mice (Fig. 2F). ISC exhaustion occurred in aging mice [47]. Nevertheless, mRNA levels of the markers of ISCs (*Lgr5* and *Ascl2*) were upregulated in the colonic crypts (Fig. 2G) of genistein-fed mice compared to those in the colonic crypts of control mice. Collectively, these data suggest that dietary genistein ameliorates age-related gastrointestinal (GI) decline in aging mice.

### 3.3. Dietary genistein regulates the composition and SCFA production of the gut microbiota in aging mice

The precise etiology of chronic intestinal inflammation in aging organisms is currently unclear. Some evidence has indicated that the gut microbiome plays a critical role in age-related inflammation [12,13]. Therefore, the impact of genistein on the gut microbiota of aging mice (26 months old) was explored using 16 S rRNA gene sequencing. A total of 929 and 938 operational taxonomic units (OTUs) were identified in the control and genistein groups, respectively (Fig. S2A). Alpha diversity was shown by Shannon's index (a proxy for diversity that takes into account both richness and evenness). A higher Shannon's index was observed in the genistein group than in the control group (Fig. 3A). Next, the beta-diversity across mouse groups was evaluated using principal coordinates analysis (PCoA) with Bray–Curtis dissimilarity (qualitative measure). PCoA revealed a separation in the gut microbiota structure between genistein-fed mice and normal control mice (Fig. 3B). Firmicutes, Bacteroidetes, and Actinobacteriota were the predominant phyla (Fig. 3C and S2B). Genistein treatment increased the ratio of Firmicutes to Bacteroidetes (Fig. 3C). At the genus level, the fecal microbiota was dominated by *Lachnospiraceae NK4A136*, *Alloprevotella*, *Dubosiella*, and *Lactobacillus* (Fig. 3D and S2C). Next, the proportion of bacterial taxa in each group was calculated using LEfSe analysis. An increase in the amount of the genera *Lachnospiraceae NK4A136* from the family Lachnospiraceae (class Clostridia), *Lactobacillus* from the family Lactobacillaceae, *Lactobacillus johnsonii*, and *Helicobacter* was observed in the genistein group, while the other two bacterial genera, *Dubosiella* and *Alloprevotella*, were enriched in the control group (Fig. 3E and S2D).

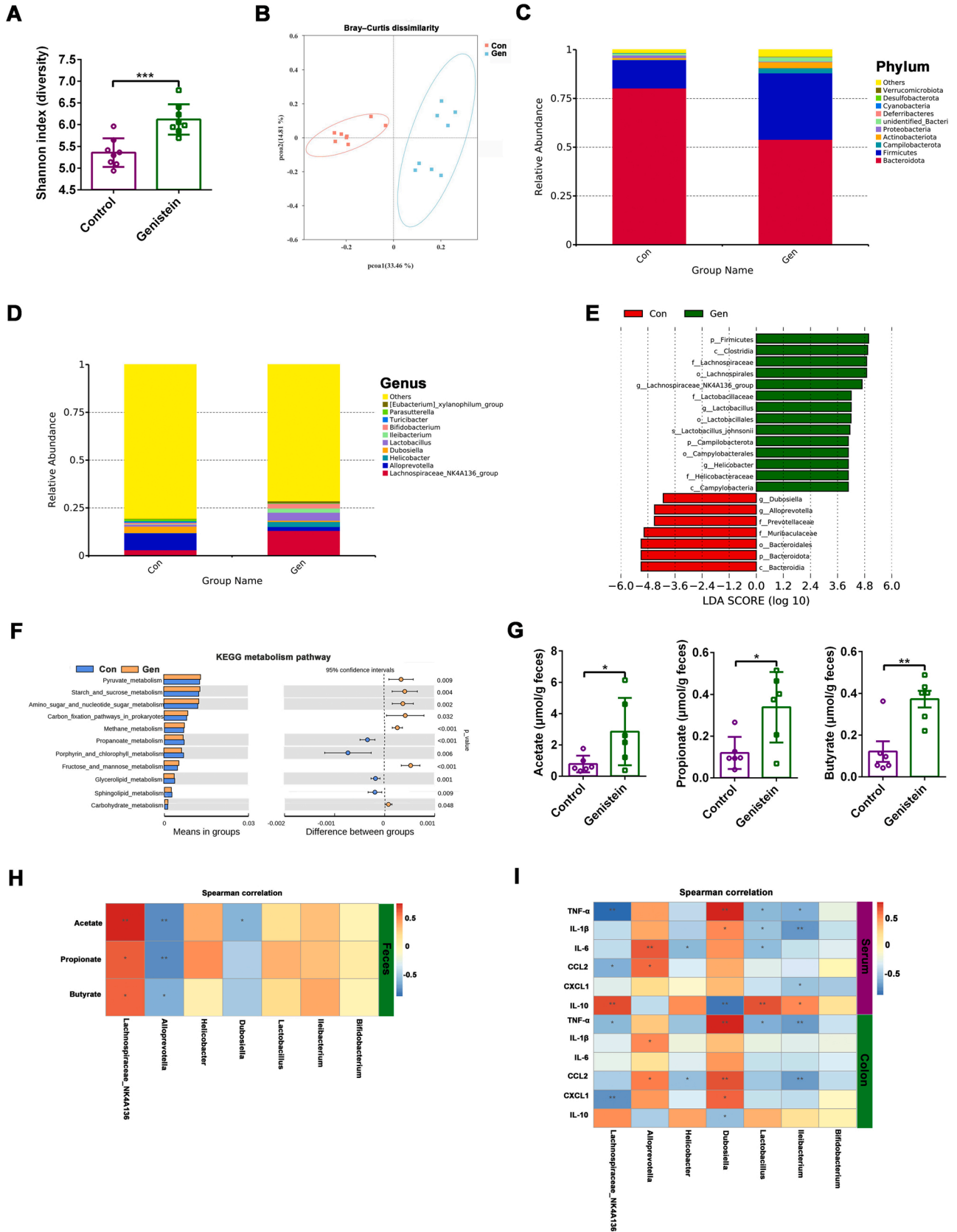
*Lachnospiraceae NK4A136* can ferment dietary polysaccharides to synthesize SCFAs in the GI tract [40,48]. SCFAs play a critical role in maintaining intestinal epithelial barrier homeostasis [49]. The KEGG enrichment analysis was predicted using 16 S rRNA sequencing results. Analysis of the KEGG metabolic pathways showed that dietary genistein principally enhanced SCFA synthesis-related metabolic pathways, including pyruvate, starch and sucrose, fructose and mannose, and carbohydrate metabolism (Fig. 3F). To further explore the effect of dietary genistein on SCFA production, the fecal concentrations of acetate, propionate, butyrate, valerate, isobutyrate, and isovalerate were measured. Notably, the production of acetate, propionate, and butyrate was increased in aging mice in response to genistein (Fig. 3G), whereas the production of the other three SCFAs was not significantly increased (Fig. S2E). Moreover, genistein enhanced the production of Lachnospiraceae-derived SCFAs (acetate, propionate, and butyrate) in vitro (Fig. S3A). Spearman's correlation analysis was performed to understand the association between differentially enriched microbes and

SCFA profiles or inflammatory parameters. Correlation analysis revealed that Lachnospiraceae *NK4A136* was enriched in the genistein group and had a strong positive correlation with the levels of SCFAs in the feces and IL-10 in the colon, but a significantly negative correlation with the levels of pro-inflammatory cytokines in the colon (Figs. 3H, 3I). Overall, it was evident that dietary genistein ameliorated gut dysbiosis and promoted SCFA production in the gut microbiota of aged mice.

### 3.4. The gut microbiota from genistein-fed mice extends the lifespan and rejuvenates the aging gut in progeroid mice

*Zmpste24*<sup>-/-</sup> progeria mice, characterized by gut dysbiosis and accelerated aging, are ideal models for studying the relationship between aging and the intestinal microbiota [18]. Based on the aforementioned results, it was hypothesized that genistein-mediated changes in the gut microbiota might accompany improved gut health and an extended lifespan in aging mice. To explore this possibility, an FMT was performed on four different mouse groups. Aging control mice and aging genistein-fed mice were used as microbiota donors and *Zmpste24*<sup>-/-</sup> mice (8 weeks old) were used as recipients: untransplanted *Zmpste24*<sup>-/-</sup> mice (hereafter referred to as Control); *Zmpste24*<sup>-/-</sup> mice transplanted with empty buffer (herein referred to as ET); *Zmpste24*<sup>-/-</sup> mice transplanted with fecal microbiota from aged control mice (hereafter referred to as A-FMT); *Zmpste24*<sup>-/-</sup> mice transplanted with fecal microbiota from genistein-fed mice (hereafter referred to as GA-FMT) (Fig. 4A). Mice in the GA-FMT group showed improved survival compared to mice in the control group, with a 19.2% increase in median lifespan (217 versus 182 days, respectively), 33.2% increase in maximum lifespan (293 versus 220 days, respectively), and 22.7% increase in mean lifespan (211 vs. 172 days, respectively) (Figs. 4B, 4C, and Table 2). In contrast, mice in the A-FMT group showed reduced survival compared to mice in the control group, with a 20.9% decrease in median lifespan (144 versus 182 days, respectively), 11.8% decrease in maximum lifespan (194 versus 220 days, respectively), and 29.3% decrease in mean lifespan (133 vs. 172 days, respectively) (Figs. 4B, 4C, and Table 2). Mice in the ET group did not show survival or lifespan differences when compared to mice in the control group (Figs. 4B, 4C). GA-FMT mice showed a delayed loss of body weight (Fig. 4D). Intestinal permeability, typically enhanced in aging mice, was lower in GA-FMT mice but higher in A-FMT mice than in control mice (Fig. 4E). Moreover, the inflammatory pathology in the colon was attenuated in GA-FMT mice (Fig. 4F). An increase in the levels of intestinal inflammation markers (TNF- $\alpha$  and IL-6) in the colon of A-FMT mice was also noted, which was recovered in GA-FMT mice (Fig. 4G). Surprisingly, the levels of IL-10 in the colon were increased in GA-FMT mice (Fig. 4G).

The composition of the gut microbiota in progeroid mice after A-FMT or GA-FMT was also analyzed. The number of OTUs in the Control, ET, A-FMT, and GA-FMT groups was 1072, 908, 931, and 1013, respectively (Fig. S3A). Antibiotic treatment decreased the Shannon index of intestinal microbiota in progeroid mice (Fig. 4H). Moreover, a higher Shannon index was observed in the GA-FMT group than in the A-FMT group (Fig. 4H). PCoA revealed a separation in the gut microbiota structure among the four groups (Fig. 4I). Firmicutes, Bacteroidetes, Proteobacteriota, and Actinobacteriota were the predominant phyla in the A-FMT and GA-FMT groups (Fig. 4J and S3B). At the genus level, the fecal microbiota was dominated by *Lachnospiraceae NK4A136*, *Bifidobacterium*, *Ileibacterium*, *Allobaculum*, *Dubosiella*, and *Ligilactobacillus* in the A-FMT and GA-FMT groups (Fig. 4K and S3C). Next, the proportion of each bacterial taxa in each group was calculated using LEfSe. Four bacterial genera: *Lachnospiraceae NK4A136*, *Bifidobacterium*, *Ileibacterium*, and *Ligilactobacillus*, were enriched in the GA-FMT group, whereas *Allobaculum* was enriched in the Control group (Fig. 4L and S3D). In the aforementioned studies, dietary genistein increased *Lachnospiraceae NK4A136* abundance and promoted SCFA production in the gut microbiota of aging mice. To further explore the effect of FMT on SCFA production, the fecal concentrations of the SCFAs were measured. Notably,



(caption on next page)

**Fig. 3.** Dietary genistein regulates the composition and short-chain fatty acid (SCFA) production of the gut microbiota in aging mice. (A–G) Gut microbiota analysis of aged control (26 months old) and genistein-fed (26 months old) mice ( $n = 8$ ). (A) Comparison of alpha diversity of the gut microbiota using Shannon's index (diversity). (B) Principal coordinates analysis of beta diversity using the Bray–Curtis dissimilarity metric. Each dot represents an individual mouse. PCo1 and PCo2 represent the percentage of variance explained by each coordinate. (C, D) Average relative abundance of prevalent microbiota at the phylum (C) and genus (D) levels in different groups. (E) Analysis of differences in microbial taxa shown by linear discriminant analysis effect size. (F) Analysis of differences in the Kyoto Encyclopedia of Genes and Genomes metabolic pathway. (G) Concentrations of acetate, propionate, and butyrate in feces from aged control (26 months old) and genistein-fed (26 months old) mice ( $n = 6$ ). Data are the mean  $\pm$  SD, \* $p < 0.05$ , \*\* $p < 0.01$  (two-tailed t-test). (H) Spearman's correlation between the gut microbiota and SCFAs in aged control (26 months old) and genistein-fed (26 months old) mice. Red denotes a positive correlation, whereas blue denotes a negative correlation. The intensity of the color is proportional to the strength of Spearman's correlation; \* $p < 0.05$ , \*\* $p < 0.01$ . (I) Spearman's correlation between the gut microbiota and cytokines in the serum or colon of the *Zmpste24*<sup>-/-</sup> mice transplanted with fecal microbiota from aged control mice and *Zmpste24*<sup>-/-</sup> mice transplanted with fecal microbiota from genistein-fed mice. Red denotes a positive correlation, whereas blue denotes a negative correlation. The intensity of the color is proportional to the strength of the Spearman's correlation; \* $p < 0.05$ , \*\* $p < 0.01$ .

the production of acetate, propionate, butyrate, and isobutyrate increased in the GA-FMT group (Fig. 4M, S3E). Spearman's correlation analysis was performed to understand the association between differentially enriched microbes and SCFA profiles or inflammatory parameters. Correlation analysis revealed that *Lachnospiraceae NK4A136* and *Bifidobacterium* enriched in the GA-FMT group had a strong positive correlation with lifespan, SCFA levels in feces, and IL-10 levels in the colon, but a significantly negative correlation with TNF- $\alpha$  and IL-6 levels in the colon (Fig. 4N).

To investigate more stringently the contribution of the microbiota to healthy aging, a “co-housing” experiment was performed. Fecal microbiota samples were passively transferred from genistein-fed aging mice through a dirty cage-sharing experiment (Fig. S5A). A traditional co-housing approach with young *Zmpste24*<sup>-/-</sup> progeria mice may lead to fighting and injury in older mice. Instead, dirty cages containing fecal material and bedding from genistein-fed or age-matched control aging mice were used to house *Zmpste24*<sup>-/-</sup> progeria mice. Consistent with the FMT experiment, mice in the Gen-Recip group showed improved survival compared to mice in the Con-No dirty cage group, with a 30.3% increase in median lifespan (224 versus 168 days, respectively), a 38.7% increase in maximum lifespan (301 versus 217 days, respectively), and a 35.6% increase in mean lifespan (221 versus 163 days, respectively) (Fig. S5B, S5C, and Table 3). In contrast, mice in the Con-Recip group showed reduced survival compared to mice in the Con-No dirty cage group, with a 14.3% decrease in median lifespan (144 versus 168 days, respectively), a 16.1% decrease in maximum lifespan (182 versus 217 days, respectively), and a 16.0% decrease in mean lifespan (163 vs. 221 days, respectively) (Fig. S5B, S5C, and Table 3). Gen-Recip mice showed a delayed loss of body weight (Fig. S5D). Consistent with the genistein-fed experiments, these results demonstrated that the gut microbiota alleviated aging-related phenotypes in genistein-fed aging mice.

### 3.5. Genistein-associated SCFAs protect TNF- $\alpha$ -induced intestinal organoid damage

Gut microbiota-derived SCFAs exert many beneficial effects on the intestinal epithelial barrier [50]. It was found that genistein or the gut microbiota of genistein-fed mice promoted the enrichment of SCFA-producing bacteria and the production of SCFAs in aging or progeroid mice, respectively. These findings prompted the investigation of how genistein ameliorates the dysfunction of the aging gut. TNF- $\alpha$ -treated colonic organoids were used to simulate inflammatory gut aging in vitro. The dose selection of acetate (1 mM), propionate (1 mM), and butyrate (1 mM) in vitro was based on the physiological concentration of each metabolite detected in the intestinal contents. The results indicated that these concentrations in the feces were 0.5–3, 0.2–0.6, and 0.2–0.7 mM, respectively (Figs. 3G, 4M). In addition, the physiological concentration of acetate, propionate, and butyrate in the colonic lumen of mice was approximately 1 mM, as reported previously [51]. The doses of SCFAs used in other studies were also referred to [52, 53]. It was found that TNF- $\alpha$  treatment led to the disruption of normal organoid morphology (Fig. 5A), upregulation of cellular senescence marker genes (*P16* and *P21*) (Fig. 5B), more apoptotic cells (Fig. 5C),

and fewer proliferating cells (Fig. 5D) compared to the control group. Interestingly, genistein had no effect on ameliorating TNF- $\alpha$ -induced organoid damage, as it did not protect normal organoid morphology, intestinal epithelial apoptosis and proliferation, or cellular senescence (Fig. 5A–5D). Instead, SCFA (propionate and butyrate) treatment protected intestinal organoids from TNF- $\alpha$ -induced damage, allowing them to maintain normal morphology (Fig. 5A). Moreover, propionate and butyrate treatment downregulated the mRNA levels of *p16* and *p21* in TNF- $\alpha$ -treated organoids (Fig. 5B). It was also noted that propionate and butyrate treatment induced more Annexin V<sup>+</sup>PI live cells and EdU<sup>+</sup> proliferating cells in TNF- $\alpha$ -treated organoids (Fig. 5C, 5D). Overall, by using the intestinal organoid model, it was demonstrated that the beneficial effects of genistein on the intestinal epithelial barrier are mediated to some extent by gut microbiota-derived SCFAs.

### 3.6. Propionate-mediated enhancement of *T*<sub>reg</sub> cell function alleviates macrophage-derived inflammation

Previous studies have demonstrated that IL-10 is a key anti-inflammatory cytokine produced by activated immune cells and has the potential to defer organism aging [7,54]. Here, it was confirmed that genistein enhanced IL-10 production in both the serum and colonic tissues of aging mice. These findings raise the question of how genistein accelerates IL-10 production in aging guts. IL-10 is expressed by many gut resident immune cells, including T cells, B cells, dendritic cells, and macrophages [55]. Here, it was found that genistein increased the frequency of IL-10-secreting colonic LPLs in aged mice (Fig. 6A). Subsequently, the frequency of IL-10-secreting CD11b<sup>+</sup> macrophages, CD11c<sup>+</sup> dendritic cells, CD19<sup>+</sup> B cells, and CD4<sup>+</sup> T cells was detected in the colonic LP. It was found that genistein did not alter the frequency of IL-10<sup>+</sup> macrophages, dendritic cells, and B cells in the colonic LP (Fig. 6A). Interestingly, the frequency of IL-10<sup>+</sup> cytokines increased in CD4<sup>+</sup> T cells in the colonic LP (Fig. 6A). In the intestinal mucosa, IL-10 is mainly produced by CD4<sup>+</sup> T cells, including T helper 2 (T<sub>H</sub>2), T<sub>H</sub>17, and T<sub>reg</sub> cells. Subsequently, the frequency of IL-10-secreting CD4<sup>+</sup>GATA-3<sup>+</sup>T<sub>H</sub>2, CD4<sup>+</sup>ROR $\gamma$ t<sup>+</sup>T<sub>H</sub>17, and CD4<sup>+</sup>CD25<sup>+</sup>T<sub>reg</sub> cells from the colonic LP was detected in aging mice (Fig. 6B). Genistein did not alter the frequency of IL-10<sup>+</sup> T<sub>H</sub>2 and IL-10<sup>+</sup> T<sub>H</sub>17 cells (Fig. 6B); however, it increased the number of IL-10<sup>+</sup> T<sub>reg</sub> cells (Fig. 6B). To investigate the mechanism involved in the increase in T<sub>reg</sub> cell-derived IL-10 induced by genistein, T<sub>reg</sub> cells from colonic LPs were sorted and stimulated in vitro with genistein and genistein-associated SCFAs (acetate, propionate, and butyrate). Notably, only propionate increased the number of IL-10<sup>+</sup> and EdU<sup>+</sup> T<sub>reg</sub> cells (Fig. 6C, 6D). These results demonstrated that genistein-associated propionate enhances colonic T<sub>reg</sub> cell function.

Aging-associated gut dysbiosis promotes macrophage dysfunction, favoring excessive production of macrophage-derived IL-6 and TNF- $\alpha$ , directly affecting intestinal homeostasis [15]. Here, it was confirmed that genistein ameliorates gut dysbiosis and decreases IL-6 and TNF- $\alpha$  production in the colonic tissues of aging mice. These findings raise the question of whether genistein relieves macrophage dysfunction in aging guts. In this study, it was found that dietary genistein decreased the frequency of IL-6<sup>+</sup> and TNF- $\alpha$ <sup>+</sup> CD11b<sup>+</sup> macrophages in colonic LPs in

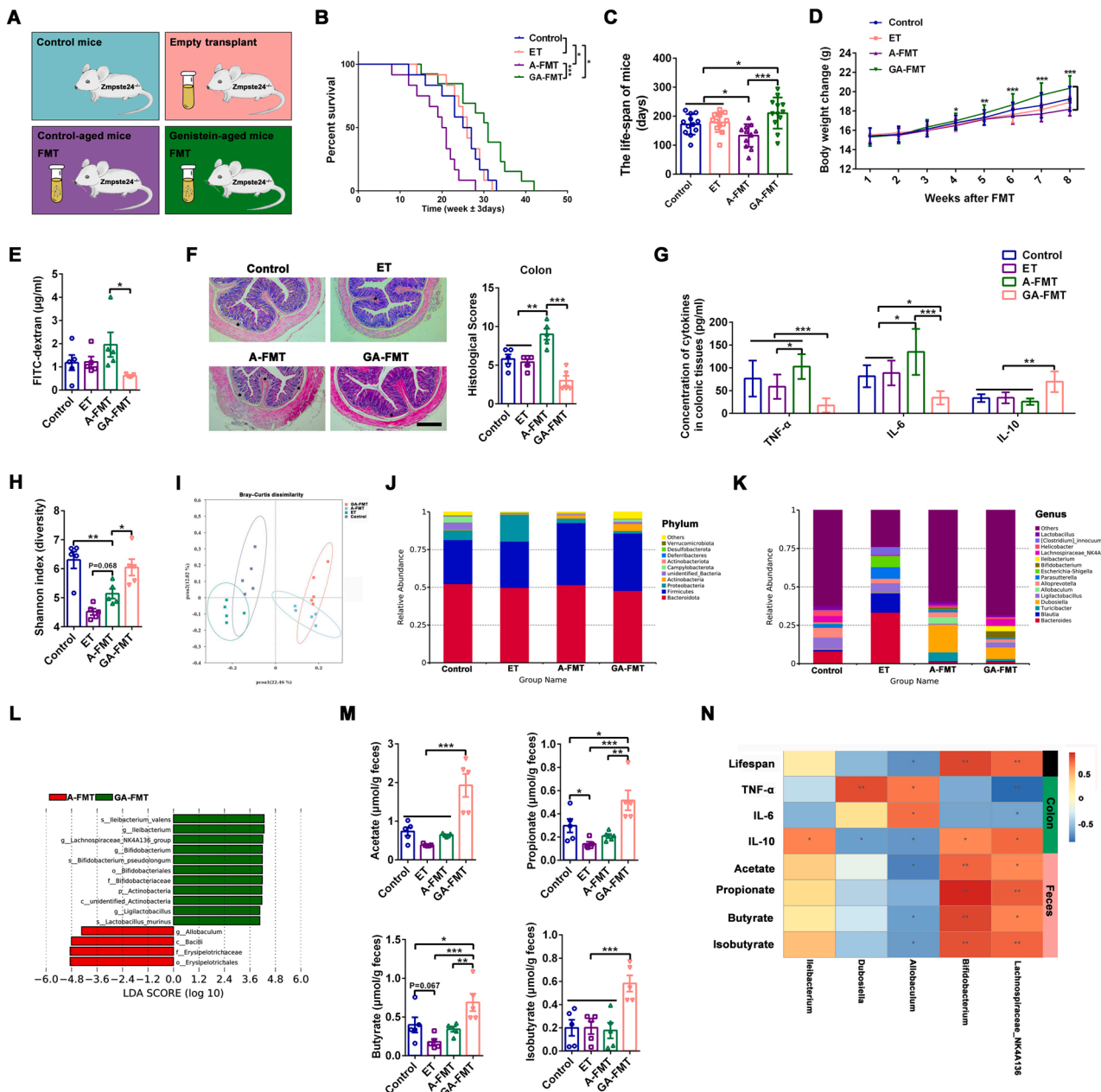


**Fig. 4.** The gut microbiota from genistein-fed mice extends the lifespan and rejuvenates the aging gut in progeroid mice. (A) Scheme of the experimental design, in which the effects of the fecal microbiota transplant (FMT) were assessed using four different groups of progeroid mice: untransplanted *Zmpste24*<sup>-/-</sup> mice (Control), *Zmpste24*<sup>-/-</sup> mice transplanted with empty buffer (ET); *Zmpste24*<sup>-/-</sup> mice transplanted with fecal microbiota from aged control (26 months old) wild-type (WT) mice (A-FMT); *Zmpste24*<sup>-/-</sup> mice transplanted with fecal microbiota from genistein-fed (26 months old) WT mice (GA-FMT). Eight-week-old *Zmpste24*<sup>-/-</sup> mice were using as recipients. (B) Percentage survival of Control, ET, A-FMT, and GA-FMT mice (n = 12). Survival curve comparisons were performed using the Log-rank test; \*p < 0.05, \*\*\*p < 0.001. (C) The lifespan of Control, ET, A-FMT, and GA-FMT mice (n = 12). Data are the mean ± standard deviation (SD), \*p < 0.05, \*\*\*p < 0.001 (one-way analysis of variance). (D) Body weight trajectories of Control, ET, A-FMT, and GA-FMT mice; n = all live animals in the study at each time point. Data are the mean ± SD, \*p < 0.05, \*\*p < 0.01, \*\*\*p < 0.001 (two-tailed t-test). (E–G) Fluorescein isothiocyanate-dextran concentration from the serum (E), representative histological images and scores of the colon; scale bar, 1000 μm (F), and the expression of cytokines (tumor necrosis factor alpha, interleukin (IL)–6, and IL-10) of the colon (G), (n = 5). Data are the mean ± SD, \*p < 0.05, \*\*p < 0.01, \*\*\*p < 0.001 (one-way analysis of variance). (H–L) Gut microbiota analysis of Control, ET, A-FMT, and GA-FMT mice (n = 5). (H) Comparison of alpha-diversity of the gut microbiota using Shannon's index (diversity). (I) Principal coordinates analysis of beta-diversity using the Bray–Curtis dissimilarity metric. Each dot represents an individual mouse. PCo1 and PCo2 represent the percentage of variance explained by each coordinate. (J, K) Average relative abundance of prevalent microbiota at the phylum (J) and genus (K) levels. (L) Taxonomic cladogram obtained from linear discriminant analysis effect size showing bacterial taxa that were differentially abundant in A-FMT and GA-FMT mice. (M) Concentrations of acetate, propionate, butyrate, and isobutyrate in feces from Control, ET, A-FMT, and GA-FMT mice (n = 5). (N) Spearman's correlation between the gut microbiota and lifespan, fecal short-chain fatty acids, or colonic cytokines in A-FMT and GA-FMT mice. The red color denotes a positive correlation, while the blue color denotes a negative correlation. The intensity of the color is proportional to the strength of Spearman's correlation; \*p < 0.05, \*\*p < 0.01.

**Table 3**  
The effect of FMT on lifespan in the dirty cage-sharing experiment.

		Median lifespan	Mean lifespan	Maximum lifespan
<i>Zmpste24</i> <sup>-/-</sup> progeroid mice	Con-No dirty cage (days)	168	163	217
	Con-Recip (days)	144	137	182
	Gen-Recip (days)	224	221	301
	Percentage extension (%; Con-Recip vs. Con-No dirty cage)	-14.3%	-16.0%	-16.1%
	Percentage extension (%; Gen-Recip vs. Con-No dirty cage)	30.3%	35.6%	38.7%

aging mice (Fig. 6E). It was hypothesized that the decreased inflammation in macrophages could be due to the propionate-mediated enhancement of T<sub>reg</sub> cell function. To test this, T<sub>reg</sub> cells and macrophages from colonic LPs were sorted, and a T<sub>reg</sub> cell-macrophage coculture model was built in vitro (Fig. 6F). LPS was used to induce macrophage-derived inflammation in vitro. Notably, coculture with IL-10 and T<sub>reg</sub> cells decreased the number of IL-6<sup>+</sup> macrophages (Fig. 6G). Moreover, coculture with T<sub>reg</sub> cells stimulated with propionate further reduced the frequency of IL-6<sup>+</sup> macrophages, which could be reversed by the anti-IL-10 antibody (Fig. 6G). Collectively, these data demonstrated that the beneficial effects of genistein on macrophage-derived inflammation, to some extent, are mediated by propionate-mediated enhancement of T<sub>reg</sub> cell function.

#### 4. Discussion

With the dramatic rise in the global aging population, addressing the determinants of delayed age-related decline or increased healthspan in elderly people has become an urgent matter. A large amount of evidence has shown that aging is associated with a decline in gut function at both

the organ and cellular levels, including gut dysbiosis, chronic inflammation, and leaky gut [13,14]. Age-related GI decline contributes to whole-organism frailty and mortality [56]. Therefore, rejuvenating the aging gut is a key strategy for promoting health in the elderly population. Besides lifestyle, host genetics, and environmental factors, dietary preference and gut microbiota are tightly associated with the aging process [1,57,58]. Moreover, nutrition is the major factor that shapes the host's gut microbiota throughout life [59]. Natural plant extracts have gained wide interest for their few side effects and extraordinary health benefits in aging population healthcare [60]. Genistein is an isoflavone found in almost all leguminous plants, including soybeans, fava beans, and coffee beans [24]. Genistein is known to have beneficial effects on age-related diseases, such as neurodegenerative diseases, cardiovascular diseases, and osteoporosis [29]. However, the precise role of genistein in homeostasis of the aging gut has not yet been identified. Furthermore, no studies have addressed the effects of genistein on delayed age-related decline in mammals. In the present study, a long-term feeding trial was designed to determine the effects of genistein on age-related frailty and mortality. This study also aimed to assess the consecutive effects of genistein on the gut microbiota and gut homeostasis in aging mammals.

The primary aim of clinical trials targeting human aging is to evaluate the maintenance of function and health [61]. Various FIs, such as 'Fried frailty phenotype' and 'Rockwood FI,' have been developed to quantify the human healthspan [5,62,63]. A clinically relevant FI consisting of 31 phenotypes was used to assess the healthspan of aging mice in the present study [6,7,42]. Here, it was demonstrated that genistein treatment extended lifespan and, more to the point, decreased the severity of multiple age-dependent phenotypes, including poor coat condition, fur color loss, and body weight loss, in aging mice. Genistein treatment did not improve these phenotypes; however, no significant adverse effects were detected following genistein treatment. Age-associated diseases are accompanied by chronic low-grade inflammation, which is defined as 'inflammaging' [43]. Inflammaging is characterized by increased levels of blood inflammatory markers that

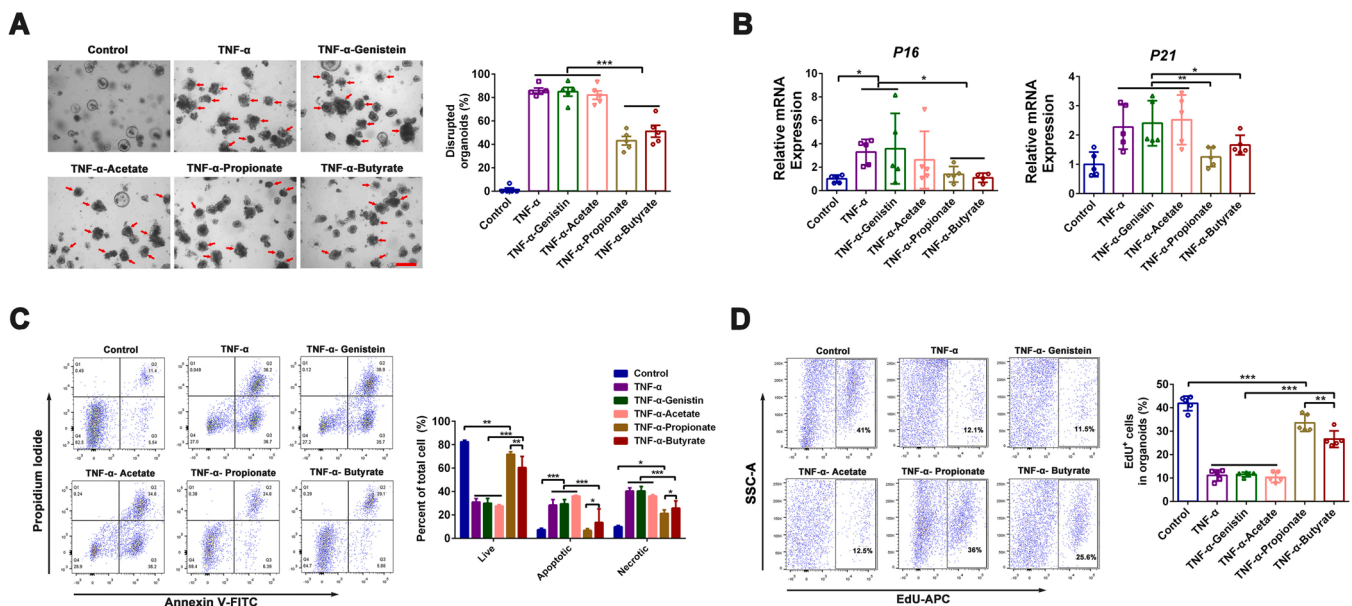
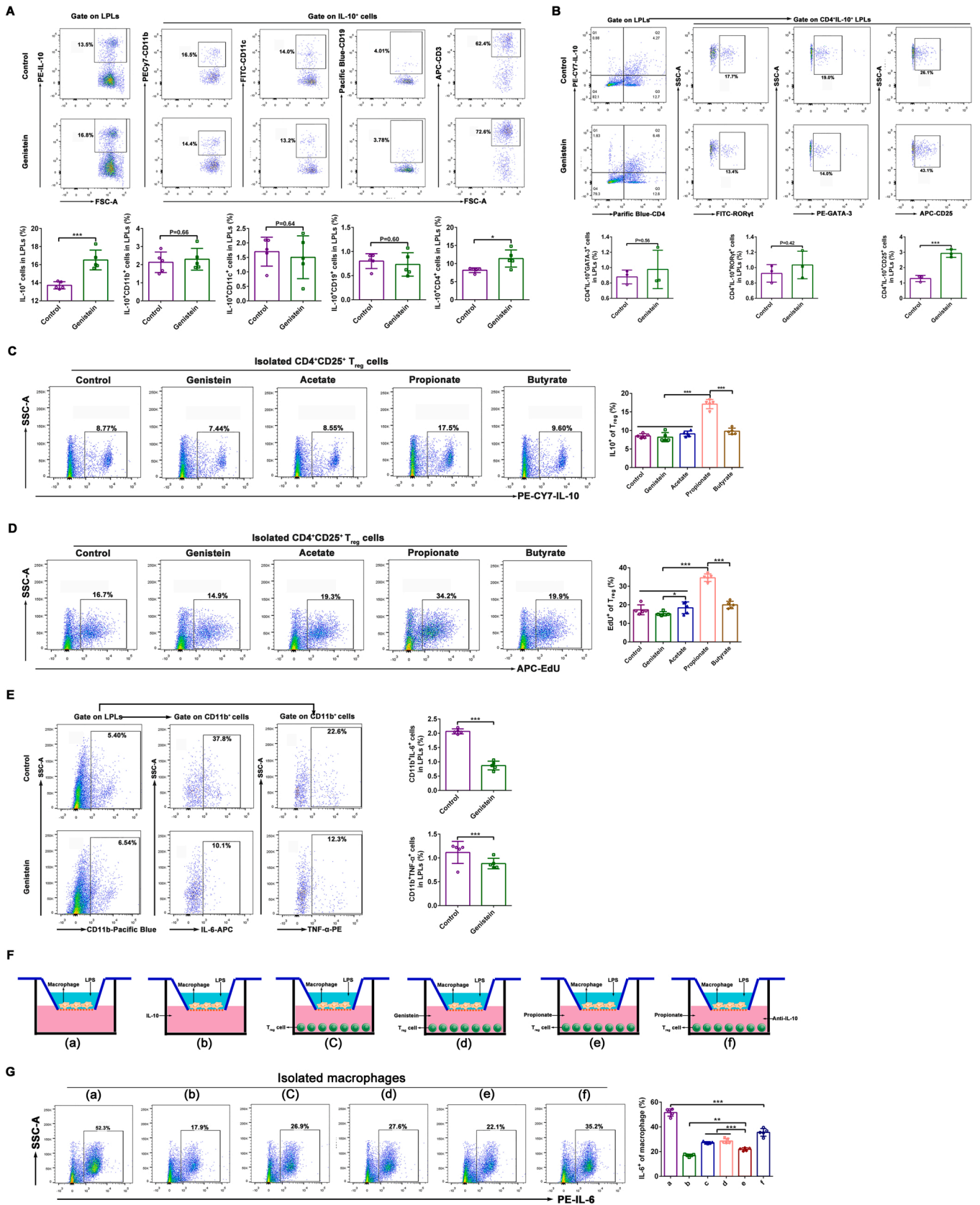


**Fig. 5.** Genistein-associated SCFAs protect against TNF- $\alpha$ -induced intestinal organoid damage. (A–D) Colonic organoids were treated with tumor necrosis factor alpha (100 ng/mL), genistein (0.1 mM), acetate (1 mM), propionate (1 mM), butyrate (1 mM), or their combinations for 24 h. (A) The morphology of the organoids in different groups was observed with a light microscope; scale bar, 200  $\mu$ m. The relative number of disrupted organoids (red arrow) in the different groups (n = 5) is shown. Data are the mean  $\pm$  standard deviation (SD), \*\*\*p < 0.001 (one-way analysis of variance). (B) qRT-PCR analysis of the markers of cellular senescence (*p16* and *p21*) of colonic organoids in different groups (n = 5). Data are the mean  $\pm$  SD, \*p < 0.05, \*\*p < 0.01, \*\*\*p < 0.001 (one-way analysis of variance). (C) Flow cytometry analysis of PI<sup>+</sup>Annexin V<sup>+</sup> (live), PI<sup>+</sup>Annexin V<sup>+</sup> (apoptotic), and PI<sup>+</sup>Annexin V<sup>+</sup> (necrotic) cell frequency of colonic organoids in different groups (n = 5). Data are the mean  $\pm$  SD, \*p < 0.05, \*\*p < 0.01, \*\*\*p < 0.001 (one-way analysis of variance). (D) Flow cytometry analysis of EdU<sup>+</sup> cell frequency of colonic organoids in different groups (n = 5). Data are the mean  $\pm$  SD, \*p < 0.05, \*\*p < 0.01, \*\*\*p < 0.001 (one-way analysis of variance).



(caption on next page)

**Fig. 6.** Propionate-mediated enhancement of regulatory T ( $T_{reg}$ ) cell function alleviates macrophage-derived inflammation. (A) Flow cytometry analysis of interleukin (IL)- $10^+$ , IL- $10^+$ CD11b $^+$  (macrophage), IL- $10^+$ CD11c $^+$  (dendritic cell), IL- $10^+$ CD19 $^+$  (B cell), and IL- $10^+$ CD4 $^+$  (T cell) frequency in colonic lamina propria lymphocytes (LPLs) of aged control (26 months old) and genistein-fed (26 months old) mice ( $n = 5$ ). Data are the mean  $\pm$  standard deviation (SD),  $*p < 0.05$ ,  $***p < 0.001$  (two-tailed t-test). (B) Flow cytometry analysis of IL- $10^+$ CD4 $^+$ GATA-3 $^+$  (Th2 cell), IL- $10^+$ CD4 $^+$ ROR $\gamma$ t $^+$  (Th17 cell), and IL- $10^+$ CD4 $^+$ CD25 $^+$  ( $T_{reg}$  cell) frequency in colonic LPLs of aged control (26 months old) and genistein-fed (26 months old) mice ( $n = 5$ ). Data are the mean  $\pm$  SD,  $***p < 0.001$  (two-tailed t-test). (C, D) Colonic  $T_{reg}$  cells were treated with genistein (0.1 mM), acetate (1 mM), propionate (1 mM), or butyrate (1 mM) for 24 h. (C) Flow cytometry analysis of colonic IL- $10^+$   $T_{reg}$  cell frequency ( $n = 5$ ). Data are the mean  $\pm$  SD,  $***p < 0.001$  (one-way analysis of variance). (D) Flow cytometry analysis of colonic EdU $^+$   $T_{reg}$  cell frequency ( $n = 5$ ). Data are the mean  $\pm$  SD,  $*p < 0.05$ ,  $***p < 0.001$  (one-way analysis of variance). (E) Flow cytometry analysis of IL-6 $^+$ CD11b $^+$  and tumor necrosis factor alpha $^+$ CD11b $^+$  frequency in colonic LPLs of aged control (26 months old) and genistein-fed (26 months old) mice ( $n = 5$ ). Data are the mean  $\pm$  SD,  $*p < 0.05$ ,  $***p < 0.001$  (two-tailed t-test). (F) Schematic of the experimental setting. Macrophages (80% confluent) of colonic LPLs were inoculated with lipopolysaccharide (1  $\mu$ g/mL) for 24 h. Next, the Transwell insert containing macrophages was cultured with IL-10 (100 ng/mL),  $T_{reg}$  cells, genistein (0.1 mM), propionate (1 mM), IL-10 antibody (1  $\mu$ g/mL), or their combination for 24 h. (G) Flow cytometry analysis of colonic IL-6 $^+$  macrophage frequency ( $n = 5$ ). Data are the mean  $\pm$  SD,  $***p < 0.001$  (one-way analysis of variance).

are highly susceptible to chronic frailty, morbidity, and premature death [11]. Consistent with previous reports [64,65], here, it was found that aged mice had significantly higher levels of blood inflammatory markers. However, 8 months of genistein treatment decreased the levels of pro-inflammatory cytokines in the serum of aging mice. Notably, genistein administration started at 18 months of age. This is valuable, as human clinical studies are likely to be initiated at a similar relative age. If translated to humans, this effect would be highly desirable as it would not only extend the lifespan, but, more importantly, reduce the debilitating period of functional decline and disease management.

Homeostasis of the intestinal barrier is closely related to the health status, defense system, and nutrition of the host [12]. However, a large amount of evidence has shown that intestinal barrier functions decline in elderly people, including intestinal inflammation, leaky gut, ISC exhaustion, and impaired epithelial regeneration [12,14]. Consistent with previous studies, here, it was found that the integrity of the intestinal barrier was impaired in aging mice. Senescent cells occur in different tissues of aging mammals and contribute to age-associated inflammation, and their removal extends the lifespan [66,67]. In this study, no consistent significant decrease in the levels of *p16* and *p21* were observed in the heart, liver, lungs, and kidneys of genistein-fed aged mice. However, genistein treatment downregulated the levels of *p16* and *p21* in the colon. Moreover, dietary genistein decreased intestinal permeability and inflammation in genistein-fed aging mice compared with age-matched controls. The mucus layer overlying the epithelium is secreted by goblet cells, which represent the first line of defense against physical and chemical injury [45]. The expression of *Muc2* in the colon was increased in genistein-fed aging mice. The intestine is constantly challenged and requires a high renewal rate that relies on *Lgr5* $^+$  ISCs to replace damaged cells to maintain its barrier function [46]. ISC exhaustion occurs in aging mice [47]. Interestingly, genistein promotes ISC-mediated intestinal epithelial renewal in elderly animals. Collectively, these results suggest that dietary genistein improves the intestinal barrier function in aging mice.

Over the last few decades, emerging evidence has shown that the gut microbiota plays a critical role in health and disease in elderly people [12,13]. Age-related changes in gut microbiota composition include a decline in microbiota diversity, decreased abundance of beneficial microorganisms, increased abundance of potential pathogenic bacteria, and an increase in the ratio of *Bacteroides* to *Firmicutes* [12,17]. It has previously been reported that dietary genistein increases the abundance of *Lactobacillus* and *Lachnospiraceae* and SCFA production in animal models and humans [27, 68–70]. Moreover, the aging gut microbiota shows a loss of genes involved in the production of SCFAs and secondary bile acids; a reduced representation of starch, sucrose, galactose, glycolysis, and gluconeogenesis metabolism pathways; and a concomitant loss of cellulolytic microorganisms [12,18]. In this study, a consistent significant increase in microbiota diversity; the abundance of *Lachnospiraceae*, *Lactobacillus*, and *Bifidobacterium*; and the ratio of *Firmicutes* to *Bacteroides* was observed in genistein-fed aging mice compared with age-matched controls. *Lachnospiraceae* has the ability to ferment dietary polysaccharides to synthesize SCFAs in the intestine [40,

48]. SCFAs play a critical role in maintaining intestinal epithelial barrier homeostasis [49]. Evidence has shown that *Lachnospiraceae* could be a universal signature of longevity and a healthy microbiome [71]. A recent study showed that *Lachnospiraceae* could protect against chemotherapy-induced gut injury, aging-like frailty, and mortality [40]. Here, it was found that dietary genistein significantly enhanced SCFA synthesis-related metabolic pathways in the gut microbiota and subsequently promoted SCFA production. Moreover, correlation analysis suggested that the relative abundance of *Lachnospiraceae* was positively correlated with the production of SCFAs and anti-inflammatory cytokines, but negatively correlated with pro-inflammatory cytokines. These outcomes indicated that the altered gut microbiota and its metabolites derived from genistein intervention may play a central role in the improvement of age-associated frailty and gut dysfunction.

Based on the aforementioned results, here, it was hypothesized that genistein-mediated changes in the gut microbiota might accompany improved intestinal homeostasis and an extended healthspan and lifespan in aging mice. To explore this possibility, *Zmpste24* $^{-/-}$  progeria mice were used as recipients, and a FMT from normal controls or genistein-fed aging mice was performed. *Zmpste24* $^{-/-}$  progeria mice, which are characterized by gut dysbiosis and accelerated aging, are ideal models for studying the relationship between healthspan and gut microbiota [18]. Interestingly, the gut microbiota from control donors shortened the lifespan and increased intestinal permeability and inflammation in progeria mice. In contrast, the gut microbiota from genistein-fed donors to progeroid recipients increased survival and improved intestinal barrier function. The composition of the gut microbiota in progeroid mice after A-FMT or GA-FMT was also analyzed. Antibiotic treatment significantly reduced bacterial diversity in progeroid mice, indicating that antibiotics cleared the gut microbiota of mice to some extent. Moreover, GA-FMT induced a significant increase in the microbiota diversity and the ratio of *Firmicutes* to *Bacteroides*. Consistent with the genistein-fed experiments, enriched *Lachnospiraceae* *NK4A136* and increased SCFA production were induced by GA-FMT. Moreover, *Lachnospiraceae* *NK4A136* enriched in the GA-FMT group had a strong positive correlation with the levels of SCFAs in the feces and the level of IL-10 in the colon, but a significantly negative correlation with the levels of IL-1 $\alpha$  and IL-6 in the colon. Based on the FMT and ‘dirty cage-sharing’ experiments as well as the authors’ previous studies, the altered gut microbiota and its metabolites derived from genistein intervention have been found to play a central role in healthspan extension and aging gut health in mammals.

Many studies have indicated that genistein can alleviate inflammation, modify the gut microbiota, and improve the epithelial barrier function in several animal models of intestinal diseases [25–28]. However, the underlying mechanisms remain unclear. Here, it was found that genistein treatment promoted the enrichment of SCFA-producing bacteria and the production of SCFAs in the aging gut. Gut microbiota-derived SCFAs (acetate, propionate, and butyrate) exert many beneficial effects on intestinal homeostasis [50]. These findings prompted us to investigate how genistein ameliorates the dysfunction of the aging gut. The complex nature of the intestinal environment in

animal models renders it challenging to study the underlying mechanisms of the beneficial effects of genistein on the aging gut. In recent years, intestinal organoid culture systems have been widely used in inflammatory models and in vitro studies of intestinal epithelial function [72]. In this study, TNF- $\alpha$ -treated colonic organoids were used to simulate inflammatory gut aging in vitro. Interestingly, genistein did not ameliorate TNF- $\alpha$ -induced organoid damage. Previous studies have demonstrated that propionate and butyrate induce autophagy in intestinal epithelial cells as a protective response against cell apoptosis [73–75]. Many studies have indicated that microbial-derived propionate and butyrate promote the epithelial barrier function through the remodeling of tight junctions [76–80]. A previous study demonstrated that gut microbiota-derived propionate induced Reg3 expression in intestinal organoids and ameliorated experimental colitis in mice [53]. A recent study reported that propionate exerts protective effects against radiation-induced intestinal epithelial injury [40]. This study also demonstrated that genistein-associated SCFAs, such as propionate and butyrate, repressed epithelial inflammation in a TNF- $\alpha$ -induced intestinal organoid damage model.

Aging-associated gut dysbiosis promotes macrophage dysfunction, favoring the excessive production of macrophage-derived IL-6 and TNF- $\alpha$ , directly affecting intestinal homeostasis [15]. This study confirmed that genistein ameliorates gut dysbiosis and decreases IL-6 and TNF- $\alpha$  production in the colonic tissues of aging mice. These findings raise the question of how genistein relieves macrophage dysfunction in aging guts. In this study, it was found that dietary genistein decreased the frequency of IL-6<sup>+</sup> and TNF- $\alpha$ <sup>+</sup> CD11b<sup>+</sup> macrophages in colonic LPs in aging mice. Previous studies have demonstrated that IL-10 is a key anti-inflammatory cytokine produced by activated immune cells and has the potential to defer organism aging [7,54]. Here, it was confirmed that genistein enhanced IL-10 production in both the serum and colonic tissues of aging mice. Moreover, T<sub>reg</sub> cells were the main source of genistein, which promoted IL-10 production in vivo. Interestingly, only propionate increased the number of IL-10<sup>+</sup> and EdU<sup>+</sup> T<sub>reg</sub> cells in vitro. These results demonstrated that genistein-associated propionate enhanced colonic T<sub>reg</sub> cell function. Previous studies have reported that commensal bacteria-derived propionate regulates T<sub>reg</sub> cell function, thereby exerting anti-inflammatory effects [81,82]. Here, it was hypothesized that the decreased inflammation in macrophages could be due to the propionate-mediated enhancement of T<sub>reg</sub> cell function. To test this, T<sub>reg</sub> cells and macrophages were sorted from colonic LPs and a T<sub>reg</sub> cell-macrophage coculture model was built in vitro. LPS was used to induce macrophage-derived inflammation in vitro. Notably, coculture with IL-10 and T<sub>reg</sub> cells decreased the frequency of IL-6<sup>+</sup> macrophages. Moreover, co-culture with T<sub>reg</sub> cells stimulated propionate and further reduced the frequency of IL-6<sup>+</sup> macrophages, which could be reversed by an anti-IL-10 antibody. The results of these in vitro experiments suggested that the beneficial effects of genistein on anti-inflammatory effects, to some extent, are mediated through SCFA-producing bacteria, such as *Lachnospiraceae*, and subsequent production of functional SCFAs, such as propionate and butyrate. However, in vivo experiments treating aging mice with SCFAs will make these conclusions more robust.

## 5. Conclusions

In summary, the present study showed that dietary genistein extended the healthspan and lifespan and modulated homeostasis of the aging gut by promoting changes in the composition and metabolites of the gut microbiota, which was translated into improved intestinal barrier functions, including decreased intestinal inflammation and permeability and increased epithelial regeneration. Given the alleviated effect of the microbiota of genistein-fed aging mice on aging-related phenotypes in progeria mice, the beneficial roles of genistein in healthspan and intestinal homeostasis are believed to be mediated mainly through SCFA-producing bacteria, such as *Lachnospiraceae*, and subsequent

production of functional SCFAs. Furthermore, the mechanism by which genistein rejuvenates the aging gut was revealed at the cellular level: genistein-associated SCFAs maintain the integrity of the intestinal epithelial barrier in the inflammatory state, and propionate-mediated enhancement of T<sub>reg</sub> cell function alleviates macrophage-derived inflammation. This study provided the first data, to the authors' knowledge, to indicate that dietary genistein modulates homeostasis in the aging gut and extends the healthspan and lifespan of aging mammals. The existence of a link between genistein and the gut microbiota provides a rationale for dietary interventions against age-associated frailty and gut dysfunction. More importantly, considering the abundance of genistein in the human diet, the present study's findings point to a potential dietary intervention that would improve the quality of life of elderly people.

This study had some limitations, and further research is needed to determine the specific mechanism by which genistein regulates the microbiota function. Although the results support the longevity effects of genistein in male animals, they lack validation in female animals. Moreover, the applied FI is subjective and lacks the power to assess cognitive function and behavior. Future studies are needed to distinguish between in vivo supplementation with genistein and direct supplementation with SCFAs, such as propionate and butyrate. Another limitation is that this study lacked clinical data. There is still a long way to go to establish the safety and efficacy of genistein in clinical longevity trials.

## Funding

This work was supported by the National Key Research and Development Program of China [grant number 2022YFE0111100]; the 2115 Talent Development Program of China Agricultural University; and the Chinese Universities Scientific Fund [grant number 2022TC173].

## CRediT authorship contribution statement

**Qihang Hou:** Data curation, Formal analysis, Methodology, Writing – original draft. **Jingxi Huang:** Data curation, Formal analysis, Methodology, Writing – original draft. **Lihua Zhao:** Data curation, Software. **Xianjie Pan:** Data curation, Software. **Chaoyong Liao:** Data curation, Software. **Qiuyu Jiang:** Data curation, Software. **Jiaqi Lei:** Data curation, Software. **Fangshen Guo:** Data curation, Software. **Jian Cui:** Data curation, Software. **Yuming Guo:** Writing – review and editing. **Bingkun Zhang:** Writing – review and editing, Conceptualization, Funding acquisition, Supervision, Validation.

## Declarations of interests

None.

## Data Availability

Data will be made available on request.

## Appendix A. Supporting information

Supplementary data associated with this article can be found in the online version at [doi:10.1016/j.phrs.2023.106676](https://doi.org/10.1016/j.phrs.2023.106676).

## References

- [1] T.S. Ghosh, F. Shanahan, P.W. O'Toole, The gut microbiome as a modulator of healthy ageing, *Nat. Rev. Gastro Hepat.* (2022).
- [2] J. Campisi, P. Kapahi, G.J. Lithgow, S. Melov, J.C. Newman, E. Verdin, From discoveries in ageing research to therapeutics for healthy ageing, *Nature* 571 (7764) (2019) 183–192.
- [3] C. Lopez-Otin, L. Galluzzi, J.M.P. Freije, F. Madeo, G. Kroemer, Metabolic control of longevity, *Cell* 166 (4) (2016) 802–821.

- [4] M. Hansen, B.K. Kennedy, Does longer lifespan mean longer Healthspan? *Trends Cell Biol.* 26 (8) (2016) 565–568.
- [5] L.P. Fried, C.M. Tangen, J. Walston, A.B. Newman, C. Hirsch, J. Gottdiener, T. Seeman, R. Tracy, W.J. Kop, G. Burke, M.A. McBurnie, G. Cardiovascular, Health Study Collaborative Research, Frailty in older adults: evidence for a phenotype, *J. Gerontol. A Biol. Sci. Med. Sci.* 56 (3) (2001) M146–M156.
- [6] J.C. Whitehead, B.A. Hildebrand, M. Sun, M.R. Rockwood, A.Y. Rose, K. Rockwood, S.E. Howlett, A clinical frailty index in aging mice: comparisons with frailty index data in humans, *J. Gerontol. A Biol. Sci. Med. Sci.* 69 (6) (2014) 621–632.
- [7] A. Asadi Shahmirzadi, D. Edgar, C.Y. Liao, Y.M. Hsu, M. Lucanic, A. Asadi Shahmirzadi, C.D. Wiley, G. Gan, D.E. Kim, H.G. Kasler, C. Kuehnemann, B. Kaplowitz, D. Bhaumik, R.R. Riley, B.K. Kennedy, G.J. Lithgow, Alpha-ketoglutarate, an endogenous metabolite, extends lifespan and compresses morbidity in aging mice, *Cell Metab.* 32 (3) (2020) 447–456, e6.
- [8] H.Y. Chung, M. Cesari, S. Anton, E. Marzetti, S. Giovannini, A.Y. Seo, C. Carter, B. P. Yu, C. Leeuwenburgh, Molecular inflammation: underpinnings of aging and age-related diseases, *Ageing Res. Rev.* 8 (1) (2009) 18–30.
- [9] T. Singh, A.B. Newman, Inflammatory markers in population studies of aging, *Ageing Res. Rev.* 10 (3) (2011) 319–329.
- [10] S. Vasto, G. Candore, C.R. Balistreri, M. Caruso, G. Colonna-Romano, M. P. Grimaldi, F. Listi, D. Nuzzo, D. Lio, C. Caruso, Inflammatory networks in ageing, age-related diseases and longevity, *Mech. Ageing Dev.* 128 (1) (2007) 83–91.
- [11] L. Ferrucci, E. Fabbri, Inflammaging: chronic inflammation in ageing, cardiovascular disease, and frailty, *Nat. Rev. Cardiol.* 15 (9) (2018) 505–522.
- [12] R. An, E. Wilms, A.A.M. Masclée, H. Smidt, E.G. Zoetendal, D. Jonkers, Age-dependent changes in GI physiology and microbiota: time to reconsider? *Gut* 67 (12) (2018) 2213–2222.
- [13] T.W. Buford, (Dis)Trust your gut: the gut microbiome in age-related inflammation, health, and disease, *Microbiome* 5 (1) (2017) 80.
- [14] J.J.V. Branca, M. Gulisano, C. Nicoletti, Intestinal epithelial barrier functions in ageing, *Ageing Res. Rev.* 54 (2019), 100938.
- [15] N. Thevaranjan, A. Puchta, C. Schulz, A. Naidoo, J.C. Szamosi, C.P. Verschoor, D. Loukov, L.P. Schenck, J. Jury, K.P. Foley, J.D. Schertzer, M.J. Larche, D. J. Davidson, E.F. Verdu, M.G. Surette, D.M.E. Bowdish, Age-associated microbial dysbiosis promotes intestinal permeability, systemic inflammation, and macrophage dysfunction, *Cell Host Microbe* 23 (4) (2018) 570.
- [16] J.W. Arnold, J. Roach, S. Fabela, E. Moorfield, S. Ding, E. Blue, S. Dagher, S. Magnus, R. Tamayo, J.M. Bruno-Barcena, M.A. Azcarate-Peril, Correction to: the pleiotropic effects of prebiotic galacto-oligosaccharides on the aging gut, *Microbiome* 9 (1) (2021) 56.
- [17] A.M. Vaiserman, A.K. Koliada, F. Marotta, Gut microbiota: a player in aging and a target for anti-aging intervention, *Ageing Res. Rev.* 35 (2017) 36–45.
- [18] C. Barcena, R. Valdes-Mas, P. Mayoral, C. Garabaya, S. Durand, F. Rodriguez, M. T. Fernandez-Garcia, N. Salazar, A.M. Nogaacka, N. Garatachea, N. Bossut, F. Arahamian, A. Lucia, G. Kroemer, J.M.P. Freije, P.M. Quiros, C. Lopez-Otin, Healthspan and lifespan extension by fecal microbiota transplantation into progeroid mice, *Nat. Med.* 25 (8) (2019) 1234–1242.
- [19] J. Martel, D.M. Ojcius, Y.F. Ko, P.Y. Ke, C.Y. Wu, H.H. Peng, J.D. Young, Hormetic effects of phytochemicals on health and longevity, *Trends Endocrinol. Metab.* 30 (6) (2019) 335–346.
- [20] F. Rivas, C. Poblete-Aro, M.E. Pando, M.J. Allel, V. Fernandez, A. Soto, P. Nova, D. Garcia-Diaz, Effects of polyphenols in aging and neurodegeneration associated with oxidative stress, *Curr. Med. Chem.* 29 (6) (2022) 1045–1060.
- [21] Z. Cui, X. Zhao, F.K. Amevor, X. Du, Y. Wang, D. Li, G. Shu, Y. Tian, X. Zhao, Therapeutic application of quercetin in aging-related diseases: SIRT1 as a potential mechanism, *Front Immunol.* 13 (2022), 943321.
- [22] D.D. Zhou, M. Luo, S.Y. Huang, A. Saimaiti, A. Shang, R.Y. Gan, H.B. Li, Effects and mechanisms of resveratrol on aging and age-related diseases, *Oxid. Med. Cell Longev.* 2021 (2021) 9932218.
- [23] B. Wang, X. Tang, B. Mao, Q. Zhang, F. Tian, J. Zhao, S. Cui, W. Chen, Anti-aging effects and mechanisms of anthocyanins and their intestinal microflora metabolites, *Crit. Rev. Food Sci. Nutr.* (2022) 1–17.
- [24] N. Jaiswal, J. Akhtar, S.P. Singh, Badruddeen, F. Ahsan, An overview on genistein and its various formulations, *Drug Res.* 69 (6) (2019) 305–313.
- [25] J. Zhang, Z. Pang, Y. Zhang, J. Liu, Z. Wang, C. Xu, L. He, W. Li, K. Zhang, W. Zhang, S. Wang, C. Zhang, Q. Hao, Y. Zhang, M. Li, Z. Li, Genistein from fructus sophorae protects mice from radiation-induced intestinal injury, *Front Pharm.* 12 (2021), 655652.
- [26] M. Zhang, J. Kou, Y. Wu, M. Wang, X. Zhou, Y. Yang, Z. Wu, Dietary genistein supplementation improves intestinal mucosal barrier function in *Escherichia coli* O78-challenged broilers, *J. Nutr. Biochem.* 77 (2020), 108267.
- [27] Y. He, H. Ayansola, Q. Hou, C. Liao, J. Lei, Y. Lai, Q. Jiang, H. Masatoshi, B. Zhang, Genistein inhibits colonic goblet cell loss and colorectal inflammation induced by salmonella typhimurium infection, *Mol. Nutr. Food Res.* 65 (16) (2021), e2100209.
- [28] N.L. Vanden Braber, I. Novotny Nunez, L. Bohl, C. Porporatto, F.N. Nazar, M. A. Montenegro, S.G. Correa, Soy genistein administered in soluble chitosan microcapsules maintains antioxidant activity and limits intestinal inflammation, *J. Nutr. Biochem.* 62 (2018) 50–58.
- [29] C. Mas-Bargues, C. Borrás, J. Vina, Genistein, a tool for geroscience, *Mech. Ageing Dev.* 204 (2022), 111665.
- [30] L. Fontana, L. Partridge, Promoting health and longevity through diet: from model organisms to humans, *Cell* 161 (1) (2015) 106–118.
- [31] E.B. Lee, D. Ahn, B.J. Kim, S.Y. Lee, H.W. Seo, Y.S. Cha, H. Jeon, J.S. Eun, D.S. Cha, D.K. Kim, Genistein from *vigna angularis* extends lifespan in *Caenorhabditis elegans*, *Biomol. Ther.* 23 (1) (2015) 77–83.
- [32] D. Altun, H. Uysal, H. Askin, A. Ayar, Determination of the effects of genistein on the longevity of *Drosophila melanogaster meigen* (Diptera: Drosophilidae), *Bull. Environ. Contam. Toxicol.* 86 (1) (2011) 120–123.
- [33] S.J. Mitchell, M. Scheibye-Knudsen, D.L. Longo, R. de Cabo, Animal models of aging research: implications for human aging and age-related diseases, *Annu Rev. Anim. Biosci.* 3 (2015) 283–303.
- [34] P. Smith, N.E. Mangan, C.M. Walsh, R.E. Fallon, A.N. McKenzie, N. van Rooijen, P. G. Fallon, Infection with a helminth parasite prevents experimental colitis via a macrophage-mediated mechanism, *J. Immunol.* 178 (7) (2007) 4557–4566.
- [35] Q. Hou, J. Huang, X. Xiong, Y. Guo, B. Zhang, Role of nutrient-sensing receptor GPRC6A in regulating colonic group 3 innate lymphoid cells and inflamed mucosal healing, *J. Crohns Colitis* (2022).
- [36] P.Y. Tsai, B. Zhang, W.Q. He, J.M. Zha, M.A. Odenwald, G. Singh, A. Tamura, L. Shen, A. Sailer, S. Yeruva, W.T. Kuo, Y.X. Fu, S. Tsukita, J.R. Turner, IL-22 upregulates epithelial claudin-2 to drive diarrhea and enteric pathogen clearance, *Cell Host Microbe* 21 (6) (2017) 671–681, e4.
- [37] E. Bolyen, J.R. Rideout, M.R. Dillon, N.A. Bokulich, C.C. Abnet, G.A. Al-Ghalith, H. Alexander, E.J. Alm, M. Arumugam, F. Asnicar, Y. Bai, J.E. Bisanz, K. Bittinger, A. Brejnrod, C.J. Brislawn, C.T. Brown, B.J. Callahan, A.M. Caraballo-Rodriguez, J. Chase, E.K. Cope, R. Da Silva, C. Diener, P.C. Dorrestein, G.M. Douglas, D. M. Durall, C. Duvallet, C.F. Edwardson, M. Ernst, M. Estaki, J. Fouquier, J. M. Gauglitz, S.M. Gibbons, D.L. Gibson, A. Gonzalez, K. Gorlick, J. Guo, B. Hillmann, S. Holmes, H. Holste, C. Huttenhower, G.A. Huttley, S. Janssen, A. K. Jarmusch, L. Jiang, B.D. Kaehler, K.B. Kang, C.R. Keefe, P. Keim, S.T. Kelley, D. Knights, I. Koester, T. Kosciulek, J. Kreps, M.G.I. Langille, J. Lee, R. Ley, Y. X. Liu, E. Loftfield, C. Lozupone, M. Maher, C. Marotz, B.D. Martin, D. McDonald, L.J. McIver, A.V. Melnik, J.L. Metcalf, S.C. Morgan, J.T. Morton, A.T. Naimey, J. A. Navas-Molina, L.F. Nothias, S.B. Orchanian, T. Pearson, S.L. Peoples, D. Petras, M.L. Preuss, E. Pruesse, L.B. Rasmussen, A. Rivers, M.S. Robinson 2nd, P. Rosenthal, N. Segata, M. Shaffer, A. Shiffer, R. Sinha, S.J. Song, J.R. Spear, A.D. Swafford, L. R. Thompson, P.J. Torres, P. Trinh, A. Tripathi, P.J. Turnbaugh, S. Ul-Hasan, J.J. Van der Hooft, F. Vargas, Y. Vazquez-Baeza, E. Vogtmann, M. von Hippel, W. Walters, Y. Wan, M. Wang, J. Warren, K.C. Weber, C.H.D. Williams, A. D. Willis, Z.Z. Xu, J.R. Zaneveld, Y. Zhang, Q. Zhu, R. Knight, J.G. Caporaso, Reproducible, interactive, scalable and extensible microbiome data science using QIIME 2, *Nat. Biotechnol.* 37 (8) (2019) 852–857.
- [38] N. Segata, J. Izard, L. Waldron, D. Gevers, L. Miropolsky, W.S. Garrett, C. Huttenhower, Metagenomic biomarker discovery and explanation, *Genome Biol.* 12 (6) (2011) R60.
- [39] K.P. Asshauer, B. Wemheuer, R. Daniel, P. Meinicke, Tax4Fun: predicting functional profiles from metagenomic 16S rRNA data, *Bioinformatics* 31 (17) (2015) 2882–2884.
- [40] H. Guo, W.C. Chou, Y. Lai, K. Liang, J.W. Tam, W.J. Brickey, L. Chen, N. D. Montgomery, X. Li, L.M. Bohannon, A.D. Sung, N.J. Chao, J.U. Peled, A.L. C. Gomes, M.R.M. van den Brink, M.J. French, A.N. Macintyre, G.D. Sempowski, X. Tan, R.B. Sartor, K. Lu, J.P.Y. Ting, Multi-omics analyses of radiation survivors identify radioprotective microbes and metabolites, *Science* 370 (6516) (2020).
- [41] Q. Hou, L. Ye, H. Liu, L. Huang, Q. Yang, J.R. Turner, Q. Yu, *Lactobacillus* accelerates IScs regeneration to protect the integrity of intestinal mucosa through activation of STAT3 signaling pathway induced by LPLs secretion of IL-22, *Cell Death Differ.* 25 (9) (2018) 1657–1670.
- [42] R.J. Parks, E. Fares, J.K. Macdonald, M.C. Ernst, C.J. Sinal, K. Rockwood, S. E. Howlett, A procedure for creating a frailty index based on deficit accumulation in aging mice, *J. Gerontol. A Biol. Sci. Med. Sci.* 67 (3) (2012) 217–227.
- [43] C. Franceschi, P. Garagnani, G. Vitale, M. Capri, S. Salvioli, Inflammaging and ‘Garb-aging’, *Trends Endocrinol. Metab.* 28 (3) (2017) 199–212.
- [44] V. Gorgoulis, P.D. Adams, A. Alimonti, D.C. Bennett, O. Bischof, C. Bishop, J. Campisi, M. Collado, K. Evangelou, G. Ferbeyre, J. Gil, E. Hara, V. Krizhanovsky, D. Jurk, A.B. Maier, M. Narita, L. Niedernhofer, J.F. Passos, P.D. Robbins, C. A. Schmitt, J. Sedivy, K. Vogtas, T. von Zglinicki, D. Zhou, M. Serrano, M. Demaria, Cellular Senescence: Defining a Path Forward, *Cell* 179 (4) (2019) 813–827.
- [45] G.M. Birchenough, M.E. Johansson, J.K. Gustafsson, J.H. Bergstrom, G.C. Hansson, New developments in goblet cell mucus secretion and function, *Mucosal Immunol.* 8 (4) (2015) 712–719.
- [46] H. Gehart, H. Clevers, Tales from the crypt: new insights into intestinal stem cells, *Nat. Rev. Gastroenterol. Hepatol.* 16 (1) (2019) 19–34.
- [47] H. Jasper, Intestinal stem cell aging: origins and interventions, *Annu Rev. Physiol.* 82 (2020) 203–226.
- [48] N. Reichardt, S.H. Duncan, P. Young, A. Belenguer, C. McWilliam Leitch, K.P. Scott, H.J. Flint, P. Louis, Phylogenetic distribution of three pathways for propionate production within the human gut microbiota, *ISME J.* 8 (6) (2014) 1323–1335.
- [49] D. Parada Venegas, M.K. De la Fuente, G. Landskron, M.J. Gonzalez, R. Quera, G. Dijkstra, H.J.M. Harmsen, K.N. Faber, M.A. Hermoso, Short Chain Fatty Acids (SCFAs)-Mediated Gut Epithelial and Immune Regulation and Its Relevance for Inflammatory Bowel Diseases, *Front Immunol.* 10 (2019) 277.
- [50] S. Deleu, K. Machiels, J. Raes, K. Verbeke, S. Vermeire, Short chain fatty acids and its producing organisms: an overlooked therapy for IBD? *EBioMedicine* 66 (2021), 103293.
- [51] G.E. Kaiko, S.H. Ryu, O.I. Koues, P.L. Collins, L. Solnica-Krezel, E.J. Pearce, E. L. Pearce, E.M. Oltz, T.S. Stappenbeck, The colonic crypt protects stem cells from microbiota-derived metabolites, *Cell* 165 (7) (2016) 1708–1720.
- [52] P.M. Smith, M.R. Howitt, N. Panikow, M. Michaud, C.A. Gallini, Y.M. Bohlooly, J. N. Glickman, W.S. Garrett, The microbial metabolites, short-chain fatty acids, regulate colonic Treg cell homeostasis, *Science* 341 (6145) (2013) 569–573.

- [53] D. Bajic, A. Niemann, A.K. Hillmer, R. Mejias-Luque, S. Bluemel, M. Docampo, M. C. Funk, E. Tonin, M. Boutros, B. Schnabl, D.H. Busch, T. Miki, R.M. Schmid, M.R. M. van den Brink, M. Gerhard, C.K. Stein-Thoeringer, Gut microbiota-derived propionate regulates the expression of reg3 mucosal lectins and ameliorates experimental colitis in mice, *J. Crohns Colitis* 14 (10) (2020) 1462–1472.
- [54] S. Dagdeviren, D.Y. Jung, R.H. Friedline, H.L. Noh, J.H. Kim, P.R. Patel, N. Tsitsilianos, K. Inashima, D.A. Tran, X. Hu, M.M. Loubato, S.M. Craige, J. Y. Kwon, K.W. Lee, J.K. Kim, IL-10 prevents aging-associated inflammation and insulin resistance in skeletal muscle, *FASEB J.* 31 (2) (2017) 701–710.
- [55] M. Saraiva, A. O'Garra, The regulation of IL-10 production by immune cells, *Nat. Rev. Immunol.* 10 (3) (2010) 170–181.
- [56] M.J. Saffrey, Aging of the mammalian gastrointestinal tract: a complex organ system, *Age* 36 (3) (2014) 9603.
- [57] Z. Ling, X. Liu, Y. Cheng, X. Yan, S. Wu, Gut microbiota and aging, *Crit. Rev. Food Sci. Nutr.* (2020) 1–56.
- [58] S.B. Kritchevsky, Nutrition and healthy aging, *J. Gerontol. A Biol. Sci. Med. Sci.* 71 (10) (2016) 1303–1305.
- [59] N. Zmora, J. Suez, E. Elinav, You are what you eat: diet, health and the gut microbiota, *Nat. Rev. Gastroenterol. Hepatol.* 16 (1) (2019) 35–56.
- [60] C.G. Fraga, K.D. Croft, D.O. Kennedy, F.A. Tomas-Barberan, The effects of polyphenols and other bioactives on human health, *Food Funct.* 10 (2) (2019) 514–528.
- [61] J.C. Newman, S. Milman, S.K. Hashmi, S.N. Austad, J.L. Kirkland, J.B. Halter, N. Barzilai, Strategies and challenges in clinical trials targeting human aging, *J. Gerontol. A Biol. Sci. Med. Sci.* 71 (11) (2016) 1424–1434.
- [62] K. Rockwood, X. Song, C. MacKnight, H. Bergman, D.B. Hogan, I. McDowell, A. Mitnitski, A global clinical measure of fitness and frailty in elderly people, *CMAJ* 173 (5) (2005) 489–495.
- [63] K. Rockwood, J.M. Blodgett, O. Theou, M.H. Sun, H.A. Feridooni, A. Mitnitski, R. A. Rose, J. Godin, E. Gregson, S.E. Howlett, A. Frailty, Index based on deficit accumulation quantifies mortality risk in humans and in mice, *Sci. Rep.* 7 (2017) 43068.
- [64] T.R. Hammond, C. Dufort, L. Dissing-Olesen, S. Giera, A. Young, A. Wysoker, A. J. Walker, F. Gergits, M. Segel, J. Nemes, S.E. Marsh, A. Saunders, E. Macosko, F. Ginhoux, J. Chen, R.J.M. Franklin, X. Piao, S.A. McCarroll, B. Stevens, Single-cell RNA sequencing of microglia throughout the mouse lifespan and in the injured brain reveals complex cell-state changes, *Immunity* 50 (1) (2019) 253–271.
- [65] A.J. Covarrubias, A. Kale, R. Perrone, J.A. Lopez-Dominguez, A.O. Pisco, H. G. Kasler, M.S. Schmidt, I. Heckenbach, R. Kwok, C.D. Wiley, H.S. Wong, E. Gibbs, S.S. Iyer, N. Basisty, Q. Wu, L.J. Kim, E. Silva, K. Vitangcol, K.O. Shin, Y.M. Lee, R. Riley, I. Ben-Sahra, M. Ott, B. Schilling, M. Scheibye-Knudsen, K. Ishihara, S. R. Quake, J. Newman, C. Brenner, J. Campisi, E. Verdin, Senescent cells promote tissue NAD(+) decline during ageing via the activation of CD38(+) macrophages, *Nat. Metab.* 2 (11) (2020) 1265–1283.
- [66] J. Campisi, Aging, cellular senescence, and cancer, *Annu Rev. Physiol.* 75 (2013) 685–705.
- [67] D.J. Baker, B.G. Childs, M. Durik, M.E. Wijers, C.J. Sieben, J. Zhong, R.A. Saltness, K.B. Jeganathan, G.C. Verzosa, A. Pezeshki, K. Khazaie, J.D. Miller, J.M. van Deursen, Naturally occurring p16(Ink4a)-positive cells shorten healthy lifespan, *Nature* 530 (7589) (2016) 184–189.
- [68] R. Yang, Q. Jia, S. Mehmood, S. Ma, X. Liu, Genistein ameliorates inflammation and insulin resistance through mediation of gut microbiota composition in type 2 diabetic mice, *Eur. J. Nutr.* 60 (4) (2021) 2155–2168.
- [69] B. Paul, K.J. Royston, Y. Li, M.L. Stoll, C.F. Skiboia, L.S. Wilson, S. Barnes, C. D. Morrow, T.O. Tollefsbol, Impact of genistein on the gut microbiome of humanized mice and its role in breast tumor inhibition, *PLoS One* 12 (12) (2017), e0189756.
- [70] P. De Boever, B. Deplancke, W. Verstraete, Fermentation by gut microbiota cultured in a simulator of the human intestinal microbial ecosystem is improved by supplementing a soygerm powder, *J. Nutr.* 130 (10) (2000) 2599–2606.
- [71] E.N. DeJong, M.G. Surette, D.M.E. Bowdish, The gut microbiota and unhealthy aging: disentangling cause from consequence, *Cell Host Microbe* 28 (2) (2020) 180–189.
- [72] Q. Hou, J. Huang, H. Ayansola, H. Masatoshi, B. Zhang, Intestinal stem cells and immune cell relationships: potential therapeutic targets for inflammatory bowel diseases, *Front. Immunol.* 11 (2020), 623691.
- [73] Y. Tang, Y. Chen, H. Jiang, D. Nie, Short-chain fatty acids induced autophagy serves as an adaptive strategy for retarding mitochondria-mediated apoptotic cell death, *Cell Death Differ.* 18 (4) (2011) 602–618.
- [74] J. Zhang, M. Yi, L. Zha, S. Chen, Z. Li, C. Li, M. Gong, H. Deng, X. Chu, J. Chen, Z. Zhang, L. Mao, S. Sun, Sodium butyrate induces endoplasmic reticulum stress and autophagy in colorectal cells: implications for apoptosis, *PLoS One* 11 (1) (2016), e0147218.
- [75] D.R. Donohoe, N. Garge, X. Zhang, W. Sun, T.M. O'Connell, M.K. Bunger, S. J. Bultman, The microbiome and butyrate regulate energy metabolism and autophagy in the mammalian colon, *Cell Metab.* 13 (5) (2011) 517–526.
- [76] C.J. Kelly, L. Zheng, E.L. Campbell, B. Saedi, C.C. Scholz, A.J. Bayless, K. E. Wilson, L.E. Glover, D.J. Kominsky, A. Magnuson, T.L. Weir, S.F. Ehrentraut, C. Pickel, K.A. Kuhn, J.M. Lanis, V. Nguyen, C.T. Taylor, S.P. Colgan, Crosstalk between Microbiota-Derived Short-Chain Fatty Acids and Intestinal Epithelial HIF augments tissue barrier function, *Cell Host Microbe* 17 (5) (2015) 662–671.
- [77] L. Peng, Z.R. Li, R.S. Green, I.R. Holzman, J. Lin, Butyrate enhances the intestinal barrier by facilitating tight junction assembly via activation of AMP-activated protein kinase in Caco-2 cell monolayers, *J. Nutr.* 139 (9) (2009) 1619–1625.
- [78] W. Miao, X. Wu, K. Wang, W. Wang, Y. Wang, Z. Li, J. Liu, L. Li, L. Peng, Sodium butyrate promotes reassembly of tight junctions in Caco-2 monolayers involving inhibition of MLCK/MLC2 pathway and phosphorylation of PKC $\beta$ 2, *Int J. Mol. Sci.* 17 (10) (2016).
- [79] L. Zheng, C.J. Kelly, K.D. Battista, R. Schaefer, J.M. Lanis, E.E. Alexeev, R.X. Wang, J.C. Onyiah, D.J. Kominsky, S.P. Colgan, Microbial-derived butyrate promotes epithelial barrier function through IL-10 receptor-dependent repression of claudin-2, *J. Immunol.* 199 (8) (2017) 2976–2984.
- [80] M.C. Valenzano, K. DiGiulio, J. Mercado, M. Teter, J. To, B. Ferraro, B. Mixson, I. Manley, V. Baker, B.A. Moore, J. Wertheimer, J.M. Mullin, Remodeling of tight junctions and enhancement of barrier integrity of the CACO-2 intestinal epithelial cell layer by micronutrients, *PLoS One* 10 (7) (2015), e0133926.
- [81] N. Arpaia, C. Campbell, X. Fan, S. Dikiy, J. van der Veeken, P. deRoos, H. Liu, J. R. Cross, K. Pfeffer, P.J. Coffey, A.Y. Rudensky, Metabolites produced by commensal bacteria promote peripheral regulatory T-cell generation, *Nature* 504 (7480) (2013) 451–455.
- [82] A. Duscha, B. Gisevius, S. Hirschberg, N. Yissachar, G.I. Stangl, E. Eilers, V. Bader, S. Haase, J. Kaisler, C. David, R. Schneider, R. Troisi, D. Zent, T. Hegelmaier, N. Dokalis, S. Gerstein, S. Del Mare-Roumani, S. Amidror, O. Staszewski, G. Poschmann, K. Stuhler, F. Hirche, A. Balogh, S. Kempa, P. Trager, M.M. Zaiss, J. B. Holm, M.G. Massa, H.B. Nielsen, A. Faissner, C. Lukas, S.G. Gatermann, M. Scholz, H. Przutnek, M. Prinz, S.K. Forsslund, K.F. Winkhofer, D.N. Muller, R. A. Linker, R. Gold, A. Haghikia, Propionic acid shapes the multiple sclerosis disease course by an immunomodulatory mechanism, *Cell* 180 (6) (2020) 1067–1080.